Chapter 4 The Nuclear Atom

Among his many experiments, Newton found that sunlight passing through a small opening in a window shutter could be refracted by a glass prism so that it would fall on a screen. The white sunlight thus refracted was spread into a rainbow-colored band—a spectrum. He had discovered *dispersion*, and his experimental arrangement was the prototype of the modern *spectroscope* (Figure 4-1*a*). When, 150 years later, Fraunhofer[1] dispersed sunlight using an experimental setup similar to that shown in Figure 4-1*b* to test prisms made of glasses that he had developed, he found that the solar spectrum was crossed by more than 600 narrow, or sharp, dark lines.[2] Soon after, a number of scientists observed sharp *bright* lines in the spectra of light emitted by flames, arcs, and sparks. *Spectroscopy* quickly became an important area of research.

It soon became clear that chemical elements and compounds emit three general types of spectra. *Continuous* spectra, emitted mainly by incandescent solids, show no lines at all, bright or dark, in spectroscopes of the highest possible resolving power. *Band* spectra consist of very closely packed groups of lines that appear to be continuous in instruments of low resolving power. These are emitted when small pieces of solid materials are placed in the source flame or electrodes. The *line* spectra mentioned already arise when the source contains unbound chemical elements. The lines and bands turned out to be characteristic of individual elements and chemical compounds when excited under specific conditions. Indeed, the spectra could be used as a highly sensitive test for the presence of elements and compounds. Line spectra raised an enormous theoretical problem: although classical physics could account for the existence of a continuous spectrum (if not its detailed shape, as we saw with blackbodies), it could in no way explain *why* sharp lines and bands should exist. Explaining the origin of the sharp lines and accounting for the primary features of the spectrum of hydrogen, the simplest element, was a major success of the so-called "old" quantum theory begun by Planck and Einstein and will be the main topic in this chapter. Full explanation of the lines and bands requires the later, more sophisticated quantum theory, which we will begin studying in Chapter 5.

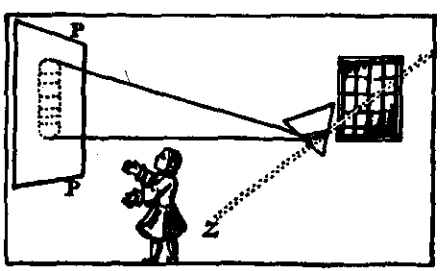

Voltaire's depiction of Newton's discovery of dispersion. [Elémens de la Philosophie de Newton, *Amsterdam, 1738.*]

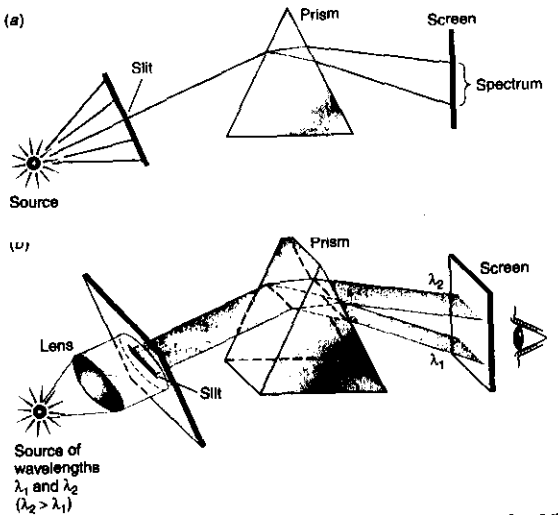

Fig. 4-1 (*a*) Light from the source passes through a small hole or a narrow slit before falling on the prism. The purpose of the slit is to ensure that all the incident light strikes the prism face at the same angle so that the dispersion by the prism causes the various frequencies that may be present to strike the screen at different places with minimum overlap. (*b*) The source emits only two wavelengths, $\lambda_2 > \lambda_1$. The source is located at the focal point of the lens so that parallel light passes through the narrow slit, projecting a narrow line onto the face of the prism. Ordinary dispersion in the prism bends the shorter wavelength through the larger total angle, separating the two wavelengths at the screen. In this arrangement each wavelength appears on the screen (or on film replacing the screen) as a narrow line, which is an image of the slit. Such a spectrum was dubbed a "line spectrum" for that reason. Prisms have been almost entirely replaced in modern spectroscopes by diffraction gratings, which have much higher resolving power.

4-1 Atomic Spectra

The characteristic radiation emitted by atoms of individual elements in a flame or in a gas excited by an electrical discharge was a subject of vigorous study during the late nineteenth century. When viewed through a spectroscope, this radiation appears as a set of discrete lines, each of a particular color or wavelength; the positions and intensities of the lines are characteristic of the element. The wavelengths of these lines could be determined with great precision, and much effort went into finding and interpreting regularities in the spectra. A major breakthrough was made in 1885 by a Swiss schoolteacher, Johann Balmer, who found that the lines in the visible and near ultraviolet spectrum of hydrogen could be represented by the empirical formula

$$\lambda_n = 364.6 \frac{n^2}{n^2 - 4} \text{ nm} \qquad 4\text{-}1$$

The uniqueness of the line spectra of the elements has enabled astronomers to determine the composition of stars, chemists to identify unknown compounds, and theme parks to have laser shows.

where n is a variable integer which takes on the values $n = 3, 4, 5, \ldots$. Figure 4-2*a* shows the set of spectral lines of hydrogen (now known as the *Balmer series*) whose wavelengths are given by Balmer's formula. For example, the wavelength of the H_α line could be found by letting $n = 3$ in Equation 4-1 (try it!), and other integers each predicted a line that was found in the spectrum. Balmer suggested that his formula might be a special case of a more general expression applicable to the spectra of other elements when ionized to a single electron, i.e., hydrogen-like elements. Such an expression, found independently by J. R. Rydberg and W. Ritz and thus called the *Rydberg-Ritz formula*, gives the reciprocal wavelength[3] as

$$\frac{1}{\lambda_{mn}} = R\left(\frac{1}{m^2} - \frac{1}{n^2}\right) \qquad \text{for} \qquad n > m \qquad \textbf{4-2}$$

where m and n are integers and R, the *Rydberg constant*, is the same for all series of spectral lines of the same element and varies only slightly, and in a regular way, from element to element. For hydrogen, the value of R is $R_H = 1.096776 \times 10^7\ \text{m}^{-1}$. For very heavy elements, R approaches the value of $R_\infty = 1.097373 \times 10^7\ \text{m}^{-1}$. Such empirical expressions were successful in predicting other spectra, such as other hydrogen lines outside the visible spectrum.

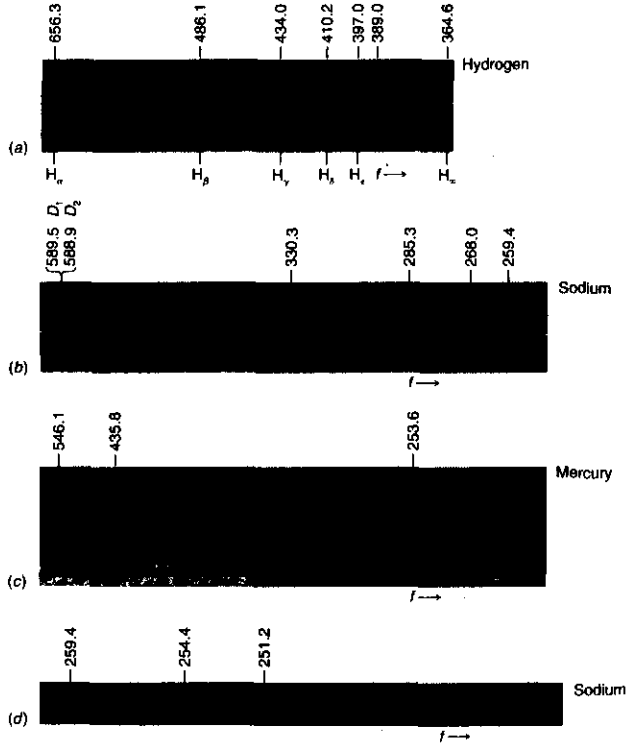

Fig. 4-2 (*a*) Emission line spectrum of hydrogen in the visible and near ultraviolet. The lines appear dark because the spectrum was photographed; hence, the bright lines are exposed (dark) areas on the film. The names of the first five lines are shown, as is the point beyond which no lines appear, H_∞, called the *limit* of the series. (*b*) A portion of the emission spectrum of sodium. The two very close bright lines at 589 nm are the D_1 and D_2 lines. They are the principal radiation from sodium street lighting. (*c*) A portion of the emission spectrum of mercury. (*d*) Part of the dark line (absorption) spectrum of sodium. White light shining through sodium vapor is absorbed at certain wavelengths, resulting in no exposure of the film at those points. Notice that the line at 259.4 nm is visible here in both the bright and dark line spectra. Note that frequency increases toward the right, wavelength toward the left in the four spectra shown.

EXAMPLE 4-1 Hydrogen Spectral Series The hydrogen Balmer series reciprocal wavelengths are those given by Equation 4-2 with $m = 2$ and $n = 3, 4, 5, \ldots$. For example, the first line of the series, H_α, would be for $m = 2, n = 3$:

$$\frac{1}{\lambda_{23}} = R\left(\frac{1}{2^2} - \frac{1}{3^2}\right) = \frac{5}{36}R = 1.523 \times 10^6\ \text{m}^{-1}$$

or

$$\lambda_{23} = 656.5\ \text{nm}$$

Other series of hydrogen spectral lines were found for $m = 1$ (by Lyman) and $m = 3$ (by Paschen). Compute the wavelengths of the first lines of the Lyman and Paschen series.

Solution

For the Lyman series ($m = 1$), the first line is for $m = 1, n = 2$.

$$\frac{1}{\lambda_{12}} = R\left(\frac{1}{1^2} - \frac{1}{2^2}\right) = \frac{3}{4}R = 8.22 \times 10^6\ \text{m}^{-1}$$

$$\lambda_{12} = 121.6\ \text{nm} \qquad \text{(in the ultraviolet)}$$

For the Paschen series ($m = 3$), the first line is for $m = 3, n = 4$:

$$\frac{1}{\lambda_{34}} = R\left(\frac{1}{3^2} - \frac{1}{4^2}\right) = \frac{7}{144}R = 5.332 \times 10^5\ \text{m}^{-1}$$

$$\lambda_{34} = 1876\ \text{nm} \qquad \text{(in the infrared)}$$

All of the lines predicted by the Rydberg-Ritz formula for the Lyman and Paschen series are found experimentally. Note that no lines are predicted to lie beyond $\lambda_\infty = 1/R = 91.2$ nm for the Lyman series and $\lambda_\infty = 9/R = 820.6$ nm for the Paschen series and none are found experimentally.

4-2 Rutherford's Nuclear Model

Many attempts were made to construct a model of the atom that yielded the Balmer and Rydberg-Ritz formulas. It was known that an atom was about 10^{-10} m in diameter, that it contained electrons much lighter than the atom, and that it was electrically neutral. The most popular model was that of J. J. Thomson, already quite successful in explaining chemical reactions. Thomson attempted various models consisting of electrons embedded in a fluid that contained most of the mass of the atom and had enough

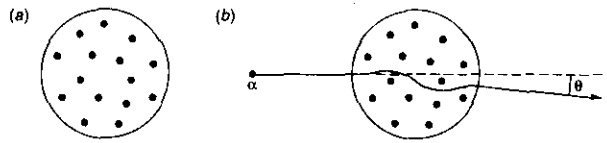

Fig. 4-3 Thomson's model of the atom: (*a*) A sphere of positive charge with electrons embedded in it so that the net charge would normally be zero. The atom shown would have been aluminum. (*b*) An α particle scattered by such an atom would have a scattering angle θ much smaller than 1°.

positive charge to make the atom electrically neutral. (See Figure 4-3*a*.) He then searched for configurations that were stable and had normal modes of vibration corresponding to the known frequency spectrum. One difficulty with all such models was that electrostatic forces alone cannot produce stable equilibrium. Thus, the charges were required to move and, if they stayed within the atom, to accelerate; however, the acceleration would result in continuous radiation, which is not observed. Despite elaborate mathematical calculations, Thomson was unable to obtain from his model a set of frequencies of vibration that corresponded with the frequencies of observed spectra.

The Thomson model of the atom was replaced by one based on the results of a set of experiments conducted by Ernest Rutherford[4] and his students H. W. Geiger and E. Marsden. Rutherford was investigating radioactivity and had shown that the radiations from uranium consisted of at least two types, which he labeled α and β. He showed, by an experiment similar to that of J. J. Thomson, that q/m for the α was half that of the proton. Suspecting that the α particles were doubly ionized helium, Rutherford and his co-workers in a classic experiment let a radioactive substance decay in a previously evacuated chamber; then, by spectroscopy, they detected the spectral lines of ordinary helium gas in the chamber. Realizing that this energetic, massive α particle would make an excellent probe for "feeling about" within the interiors of other atoms, Rutherford began a series of experiments with this purpose.

In these latter experiments, a narrow beam of α particles fell on a zinc sulfide screen, which emitted visible light scintillations when struck (Figure 4-4). The distribution of scintillations on the screen was observed when various thin metal foils were placed between it and the source. Most of the α particles were either undeflected, or deflected through very small angles of the order of 1°. Quite unexpectedly, however, a few α particles were deflected through angles as large as 90° or more. If the atom consisted of a positively charged sphere of radius 10^{-10} m, containing electrons as in the Thomson model, only a very small deflection could result from a single encounter between an α particle and an atom, even if the α particle penetrated into the atom.

Hans Geiger and Ernest Rutherford in their Manchester laboratory. [*Courtesy of University of Manchester.*]

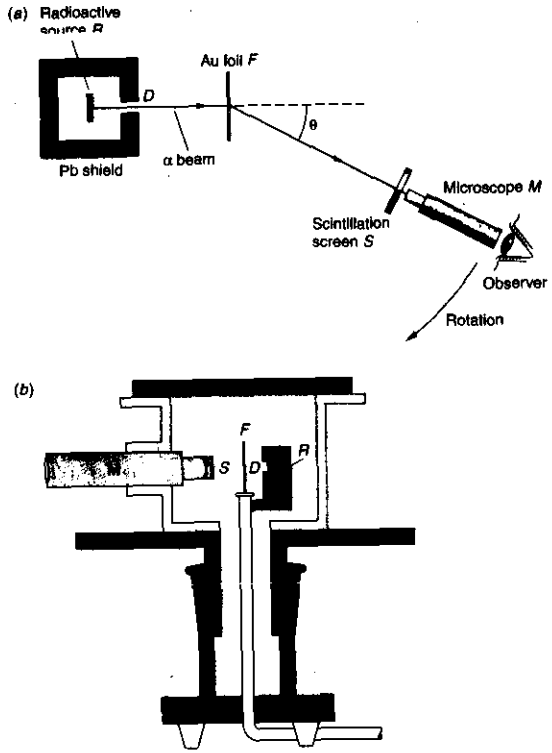

Fig. 4-4 Schematic diagram of the apparatus used by Geiger and Marsden to test Rutherford's atomic model. (*a*) The beam of α particles is defined by the small hole *D* in the shield surrounding the radioactive source *R* of ^{214}Bi (called RaC in Rutherford's day). The α beam strikes an ultrathin gold foil *F* (about 2000 atoms thick), and the α particles are individually scattered through various angles. Those scattering at the angle θ shown strike a small screen *S* coated with a scintillator, i.e., a material that emits tiny flashes of light (scintillations) when struck by an α particle. The scintillations were viewed by the observer through a small microscope *M*. The scintillation screen–microscope combination could be rotated about the center of the foil. The region traversed by the α beam is evacuated. The experiment consisted of counting the number of scintillations as a function of θ. (*b*) A diagram of the actual apparatus as it appeared in Geiger and Marsden's paper describing the results. The letter key is the same as in (*a*). [*Part (b) from H. Geiger and E. Marsden,* Philosophical Review, *25, 507 (1913).*]

Indeed, calculations showed that the Thomson atomic model could not possibly account for the number of large-angle scatterings that Rutherford saw. The unexpected scatterings at large angles were described by Rutherford with these words:

> It was quite the most incredible event that ever happened to me in my life. It was as incredible as if you fired a 15-inch shell at a piece of tissue paper and it came back and hit you.

Rutherford's Scattering Theory and the Nuclear Atom

The question is, then, Why would one obtain the large-angle scattering that Rutherford saw? The trouble with the Thomson atom is that it is too "soft"—the maximum force experienced by the α is too weak to give a large deflection. If the positive charge of the atom is concentrated in a more compact region, however, a much larger force will occur at near impacts. Rutherford concluded that the large-angle scattering obtained experimentally could result only from a single encounter of the α particle with a massive charge confined to a volume much smaller than that of the whole atom. Assuming this "nucleus" to be a point charge, he calculated the expected angular distribution for the scattered α particles. His predictions of the dependence of scattering probability on angle, nuclear charge, and kinetic energy were completely verified in a series of experiments carried out in his laboratory by Geiger and Marsden.

We shall not go through Rutherford's derivation in detail, but merely outline the assumptions and conclusions. Figure 4-5 shows the geometry of an α particle being scattered by a nucleus, which we take to be a point charge Q at the origin. Initially, the α particle approaches with speed v along a line a distance b from a parallel line COA through the origin. The force on the α particle is $F = kq_\alpha Q/r^2$, given by Coulomb's law (see Figure 4-6). After scattering, when the α particle is again far from the nucleus, it is moving with the same speed v parallel to the line OB, which makes an angle θ with line COA. (Since the potential energy is again zero, the final speed must be equal to the initial speed by conservation of energy, assuming, as Rutherford did, that the massive nucleus remains fixed during the scattering.) The distance b is called the *impact parameter*, and the angle θ, the *scattering angle*. The path of the α particle

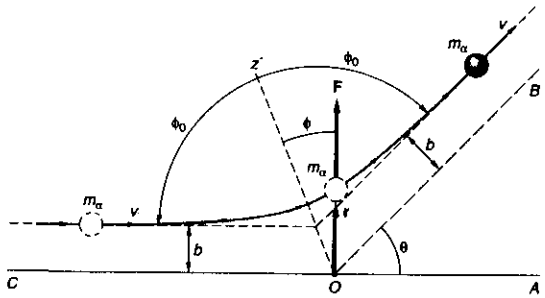

Fig. 4-5 Rutherford scattering geometry. The nucleus is assumed to be a point charge Q at the origin O. At any distance r the α particle experiences a repulsive force $kq_\alpha Q/r^2$. The α particle travels along a hyperbolic path that is initially parallel to line OA a distance b from it and finally parallel to line OB, which makes an angle θ with OA. The scattering angle θ can be related to the impact parameter b by classical mechanics.

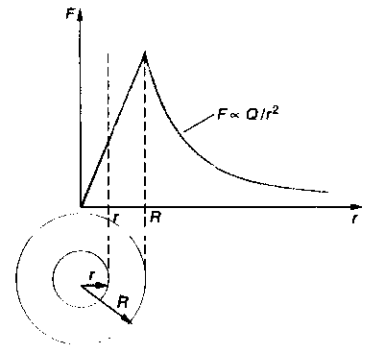

Fig. 4-6 Force on a point charge versus distance r from the center of a uniformly charged sphere of radius R. Outside the sphere the force is proportional to Q/r^2, where Q is the total charge. Inside the sphere, the force is proportional to $q'/r^2 = Qr/R^3$, where $q' = Q(r/R)^3$ is the charge within a sphere of radius r. The maximum force occurs at $r = R$.

can be shown to be a hyperbola, and the scattering angle θ can be related to the impact parameter b from the laws of classical mechanics. The result is

$$b = \frac{kq_\alpha Q}{m_\alpha v^2} \cot \frac{\theta}{2} \qquad \textbf{4-3}$$

Of course, it is not possible to choose or know the impact parameter for any α particle; but, recalling the values of the cotangent between 0° and 90°, all such particles with impact parameters less than or equal to a particular b will be scattered through an angle θ greater than or equal to that given by Equation 4-3; i.e., the smaller the impact parameter, the larger the scattering angle (Figure 4-7). Let the intensity of the incident α particle beam be I_0 particles per second per unit area. The number per second scattered by one nucleus through angles greater than θ equals the number per second that have impact parameters less than $b(\theta)$. This number is $\pi b^2 I_0$.

The quantity πb^2, which has the dimensions of an area, is called the *cross section* σ for scattering through angles greater than θ. The cross section σ is thus

The particle-scattering technique devised by Rutherford to "look" at atoms now has wide application throughout physics. Scattering of high-energy electrons from protons and neutrons provided our first experimental hint of the existence of quarks.

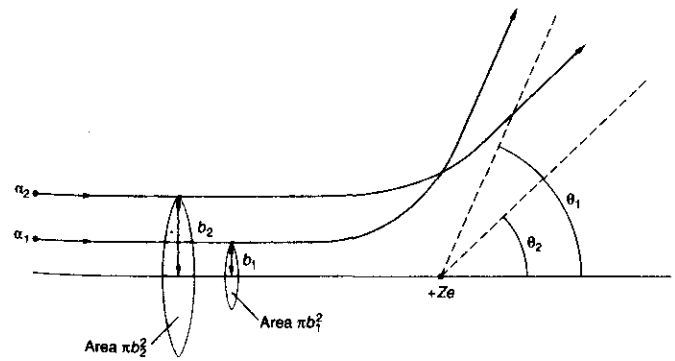

Fig. 4-7 Two α particles with equal kinetic energies approach the positive charge $Q = +Ze$ with impact parameters b_1 and b_2, where $b_1 < b_2$. According to Equation 4-3, the angle θ_1 through which α_1 is scattered will be larger than θ_2. In general, all α particles with impact parameters smaller than a particular value of b will have scattering angles larger than the corresponding value of θ from Equation 4-3. The area πb^2 is called the cross section for scattering with angles greater than θ.

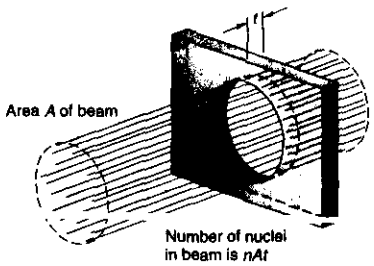

Fig. 4-8 The total number of nuclei of foil atoms in the area covered by the beam is nAt, where n is the number of foil atoms per unit volume, A is the area of the beam, and t is the thickness of the foil.

defined as the number scattered per nucleus per unit time divided by the incident intensity. The total number of particles scattered per second is obtained by multiplying $\pi b^2 I_0$ by the number of nuclei in the scattering foil (this assumes the foil to be thin enough to make the chance of overlap negligible). Let n be the number of nuclei per unit volume:

$$n = \frac{\rho(\text{g/cm}^3)\, N_A(\text{atoms/mol})}{M(\text{g/mol})} = \frac{\rho N_A}{M}\ \frac{\text{atoms}}{\text{cm}^3} \qquad \textbf{4-4}$$

For a foil of thickness t, the total number of nuclei "seen" by the beam is nAt, where A is the area of the beam (Figure 4-8). The total number scattered per second through angles greater than θ is thus $\pi b^2 I_0 ntA$. If we divide this by the number of α particles incident per second $I_0 A$, we get the fraction f scattered through angles greater than θ:

$$f = \pi b^2 nt \qquad \textbf{4-5}$$

EXAMPLE 4-2 Scattered Fraction f Calculate the fraction of an incident beam of α particles of kinetic energy 5 MeV that Geiger and Marsden expected to see for $\theta \geq 90°$ from a gold foil ($Z = 79$) 10^{-6} m thick.

Solution

1. The fraction f is related to the impact parameter b, the number density of nuclei n, and the thickness t by Equation 4-5:

$$f = \pi b^2 nt$$

2. The particle density n is given by Equation 4-4:

$$n = \frac{\rho N_A}{M} = \frac{(19.3\ \text{g/cm}^3)(6.02 \times 10^{23}\ \text{atoms/mol})}{197\ \text{g/mol}}$$
$$= 5.90 \times 10^{22}\ \text{atoms/cm}^3 = 5.90 \times 10^{28}\ \text{atoms/m}^3$$

3. The impact parameter b is related to θ by Equation 4-3:

$$b = \frac{kq_\alpha Q}{m_\alpha v^2} \cot\frac{\theta}{2} = \frac{(2)(79)\, ke^2}{2K_\alpha} \cot\frac{90°}{2}$$
$$= \frac{(2)(79)(1.44\ \text{eV}\cdot\text{nm})}{(2)(5 \times 10^6\ \text{eV})} = 2.28 \times 10^{-5}\ \text{nm}$$
$$= 2.28 \times 10^{-14}\ \text{m}$$

4. Substituting these into Equation 4-5 yields f:

$$f = \pi(2.28 \times 10^{-14}\text{m})^2\left(5.9 \times 10^{28}\ \frac{\text{atoms}}{\text{m}^3}\right)(10^{-6}\,\text{m})$$
$$= 9.6 \times 10^{-4}$$

Remarks: *This is in good agreement with Geiger and Marsden's measurement of about 1 in 8000 in their first trial. Thus, the nuclear model is in good agreement with their results.*

On the strength of the good agreement between the nuclear atomic model and the measured fraction of the incident α particles scattered at angles $\theta \geq 90°$, Rutherford derived an expression, based on the nuclear model, for the number of α particles ΔN that would be scattered at any angle θ. That number, which also depends on the atomic number Z and thickness t of the scattering foil, on the intensity I_0 of the incident α particles and their kinetic energy E_k, and on the geometry of the detector (A_{sc} is the detector area and r is the foil-detector distance), is given by

$$\Delta N = \left(\frac{I_0 A_{sc} nt}{r^2}\right)\left(\frac{kZe^2}{2E_k}\right)^2 \frac{1}{\sin^4(\theta/2)} \qquad \textbf{4-6}$$

Within the uncertainties of their experiments, which involved visually observing several hundred thousand α particles, Geiger and Marsden verified every one of the predictions of Rutherford's formula over four orders of magnitude of ΔN. The excellent agreement of their data with Equation 4-6 firmly established the nuclear atomic model as the correct basis for further studies of atomic and nuclear phenomena. (See Figure 4-12.)

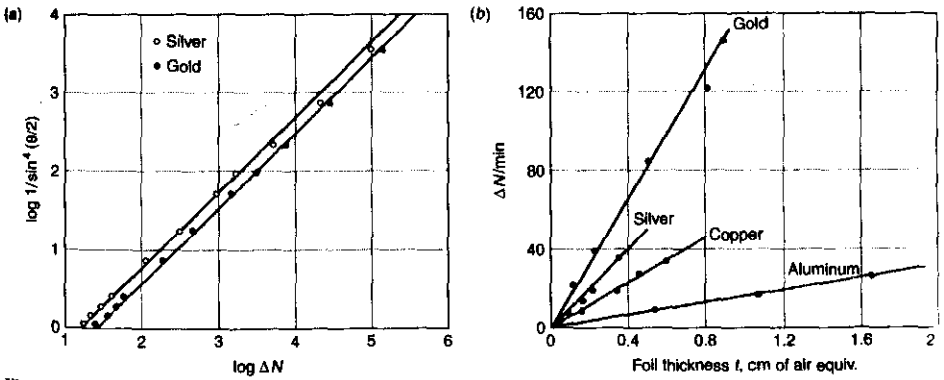

Fig. 4-12 (*a*) Geiger and Marsden's data for α scattering from thin gold and silver foils. The graph is a log-log plot to show the data over several orders of magnitude. Note that scattering angle increases downward along the vertical axis. (*b*) Geiger and Marsden also measured the dependence of ΔN on t predicted by Equation 4-6 for foils made from a wide range of elements, this being an equally critical test. Results for four of the elements used are shown.

More

Rutherford's derivation of Equation 4-6 was based on his atomic model and the well-known Coulomb scattering process of charged particles. *Rutherford's Prediction and Geiger and Marsden's Results* are described on the home page: www.whfreeman.com/modphysics4e See also Equations 4-7 through 4-10 here, as well as Figures 4-9 through 4-12.

The Size of the Nucleus

The fact that the force law is shown to be correct, confirming Rutherford's model, does not imply that the nucleus is a mathematical point charge, however. The force law would be the same even if the nucleus were a ball of charge of some radius R_0, as long as the α particle did not penetrate the ball. (See Figures 4-5 and 4-13.) For a given scattering angle, the distance of closest approach of the α particle to the nucleus can be calculated from the geometry of the collision. For the largest angle, near 180°, the collision is nearly "head-on." The corresponding distance of closest approach r_d is thus an experimental upper limit on the size of the target nucleus. We can calculate the distance of closest approach for a head-on collision r_d by noting that conservation of energy requires the potential energy at this distance to equal the original kinetic energy:

$$(V + E_k)_{\text{large } r} = (V + E_k)_{r_d}$$

$$(0 + \frac{1}{2}m_\alpha v^2)_{\text{large } r} = \left(\frac{kq_\alpha Q}{r_d} + 0\right)_{r_d}$$

$$\frac{1}{2}m_\alpha v^2 = \frac{kq_\alpha Q}{r_d}$$

or

$$r_d = \frac{kq_\alpha Q}{\frac{1}{2}m_\alpha v^2} \qquad \textbf{4-11}$$

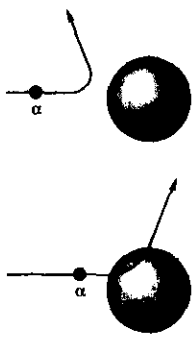

Fig. 4-13 (*a*) If the α particle does not penetrate the nuclear charge, the nucleus can be considered a point charge located at the center. (*b*) If the particle has enough energy to penetrate the nucleus, the Rutherford scattering law does not hold, but would require modification to account for that portion of the nuclear charge "behind" the penetrating α particle.

For the case of 7.7-MeV α particles, the distance of closest approach for a head-on collision is

$$r_d = \frac{(2)(79)(1.44\text{ eV}\cdot\text{nm})}{7.7 \times 10^6\text{ eV}} \approx 3 \times 10^{-5}\text{ nm} = 3 \times 10^{-14}\text{ m}$$

For other collisions, the distance of closest approach is somewhat greater, but for α particles scattered at large angles it is of the same order of magnitude. The excellent agreement of Geiger and Marsden's data at large angles with the prediction of Equation 4-6 thus indicates that the radius of the gold nucleus is no larger than about 3×10^{-14} m. If higher-energy particles could be used, the distance of closest approach would be smaller; and as the energy of the α particles increased, we might expect that eventually the particles would penetrate the nucleus. Since, in that event, the force law is no longer $F = kq_\alpha Q/r^2$, the data would not agree with the point-nucleus calculation. Rutherford

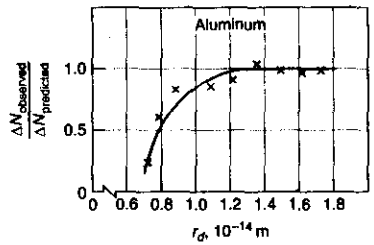

Fig. 4-14 Data from Rutherford's group showing observed α scattering at a large fixed angle versus values of r_d computed from Equation 4-11 for various kinetic energies.

did not have higher-energy α particles available, but he could reduce the distance of closest approach by using targets of lower atomic numbers.[9] For the case of aluminum, with $Z = 13$, the most energetic α particles that he had available (7.7 MeV from ^{214}Bi), scattered at large angles did not follow the predictions of Equation 4-6. However, when their kinetic energy was reduced by passing the beam through thin mica sheets of various thicknesses, the data again followed the prediction of Equation 4-6. Rutherford's data are shown in Figure 4-14. The value of r_d (calculated from Equation 4-11) at which the data begin to deviate from the prediction can be thought of as the surface of the nucleus. From these data, Rutherford estimated the radius of the aluminum nucleus to be about 1.0×10^{-14} m. (The radius of the Al nucleus is actually about 3.6×10^{-15} m. See Chap. 11.)

A unit of length convenient for describing nuclear sizes is the fermi, or femtometer (fm), defined by 1 fm = 10^{-15} m. As we shall see in Chapter 11, the nuclear radius varies from about 1 to 10 fm from the lightest to the heaviest atoms.

EXAMPLE 4-3 Rutherford Scattering at Angle θ In a particular experiment, α particles from ^{226}Ra are scattered at θ = 45° from a silver foil and 450 particles are counted each minute at the scintillation detector. If everything is kept the same except that the detector is moved to observe particles scattered at 90°, how many will be counted per minute?

Solution

Using Equation 4-6, we have that $\Delta N = 450$ when $\theta = 45°$, but we don't have any of the other parameters available. Letting all of the quantities in the parentheses equal a constant C, we have

$$\Delta N = 450 = C \sin^{-4}\left(\frac{45°}{2}\right)$$

or

$$C = 450 \sin^4\left(\frac{45°}{2}\right)$$

When the detector is moved to θ = 90°, the value of C is unchanged, so

$$\Delta N = C \sin^{-4}\left(\frac{90°}{2}\right) = 450 \sin^4\left(\frac{45°}{2}\right) \sin^{-4}\left(\frac{90°}{2}\right)$$

$$= 38.6 \approx 39 \text{ particles/min}$$

EXAMPLE 4-4 Alpha Scattering A beam of α particles with $E_k = 6.0$ MeV impinges on a silver foil 1.0 μm thick. The beam current is 1.0 nA. How many α particles will be counted by a small scintillation detector of area equal to 5 mm² located 2.0 cm from the foil at an angle of 75°? (For silver $Z = 47$, $\rho = 10.5$ gm/cm³, and $M = 108$.)

Solution

1. The number counted ΔN is given by Equation 4-6:

$$\Delta N = \left(\frac{I_0 A_{sc} nt}{r^2}\right)\left(\frac{kZe^2}{2E_k}\right)^2 \frac{1}{\sin^4(\theta/2)}$$

2. Since each α particle has $q_\alpha = 2e$, I_0 is:

$$I_0 = (1.0 \times 10^{-9}\ \text{A})(2 \times 1.60 \times 10^{-19}\ C/\alpha)^{-1}$$
$$= 3.12 \times 10^9\ \alpha/\text{s}$$

3. The kinetic energy of each α is:

$$E_k = (6.0\ \text{MeV})(1.60 \times 10^{-13}\ \text{J/MeV})$$
$$= 9.60 \times 10^{-13}\ \text{J}$$

4. For silver, n is given by:

$$n = \rho N_A / M$$
$$= \frac{(110.5\ \text{g/cm}^3)(6.02 \times 10^{23}\ \text{atoms/mol})}{108\ \text{g/mol}}$$
$$= 5.85 \times 10^{22}\ \text{atoms/cm}^3 = 5.85 \times 10^{28}\ \text{atoms/m}^3$$

5. Substituting the given values and computed results into Equation 4-6 gives ΔN:

$$\Delta N = \frac{(3.12 \times 10^9\ \alpha/\text{s})(5 \times 10^{-6}\ \text{m}^2)(5.85 \times 10^{28}\ \text{atoms/m}^3)(10^{-6}\ \text{m})}{(2 \times 10^{-2})^2 \sin^4(75°/2)}$$
$$\times \left[\frac{(9 \times 10^9)(47)(1.60 \times 10^{-19})^2}{(2)(9.60 \times 10^{-13})}\right]$$
$$= 528\ \alpha/\text{s}$$

EXAMPLE 4-5 Radius of the Au Nucleus The radius of the gold (Au) nucleus has been measured by high-energy electron scattering as 6.6 fm. What kinetic energy α particles would Rutherford have needed so that for 180° scattering, the α particle would just reach the nuclear surface before reversing direction?

Solution

From Equation 4-11, we have

$$\frac{1}{2}m_\alpha v^2 = \frac{kq_\alpha Q}{r_d} = \frac{(9 \times 10^9)(2)(79)(1.6 \times 10^{-19})^2}{6.6 \times 10^{-15}}$$
$$= 5.52 \times 10^{-12}\ \text{J} = 34.5\ \text{MeV}$$

Alpha particles of such energy are not emitted by naturally radioactive materials and hence were not accessible to Rutherford. Thus, he could not have performed an experiment for Au equivalent to that for Al illustrated by Figure 4-14.

QUESTIONS

1. Why can't the impact parameter for a particular α particle be chosen?
2. Why is it necessary to use a very thin target foil?
3. Why could Rutherford place a lower limit on the radius of the Al nucleus but not on the Au nucleus?
4. How could you use the data in Figure 4-12*a* to determine the charge on a silver nucleus relative to that on a gold nucleus?
5. How would you expect the data (not the curve) to change in Figure 4-12 if the foil were so thick that an appreciable number of gold nuclei were hidden from the beam by being in the "shadow" of the other gold nuclei?

4-3 The Bohr Model of the Hydrogen Atom

In 1913, the Danish physicist Niels H. D. Bohr[10] proposed a model of the hydrogen atom which combined the work of Planck, Einstein, and Rutherford and was remarkably successful in predicting the observed spectrum of hydrogen. The Rutherford

Niels Bohr explains a point in front of the blackboard (1956). [*American Institute of Physics, Niels Bohr Library, Margrethe Bohr Collection.*]

model assigned charge and mass to the nucleus but was silent regarding the distribution of the charge and mass of the electrons. Bohr, who had been working in Rutherford's laboratory during the experiments of Geiger and Marsden, made the assumption that the electron in the hydrogen atom moved in an orbit about the positive nucleus, bound by the electrostatic attraction of the nucleus. Classical mechanics allows circular or elliptical orbits in this system, just as in the case of the planets orbiting the sun. For simplicity, Bohr chose to consider circular orbits.

Such a model is mechanically stable, because the Coulomb potential $V = -kZe^2/r$ provides the centripetal force

$$F = \frac{kZe^2}{r^2} = \frac{mv^2}{r} \qquad \textbf{4-12}$$

necessary for the electron to move in a circle of radius r at speed v; but it is electrically unstable because the electron is always accelerating toward the center of the circle. The laws of electrodynamics predict that such an accelerating charge will radiate light of frequency f equal to that of the periodic motion, which in this case is the frequency of revolution. Thus, classically,

$$f = \frac{v}{2\pi r} = \left(\frac{kZe^2}{rm}\right)^{1/2} \frac{1}{2\pi r} = \left(\frac{kZe^2}{4\pi^2 m}\right)^{1/2} \cdot \frac{1}{r^{3/2}} \sim \frac{1}{r^{3/2}} \qquad \textbf{4-13}$$

The total energy of the electron is the sum of the kinetic and the potential energies:

$$E = \frac{1}{2}mv^2 + \left(-\frac{kZe^2}{r}\right)$$

From Equation 4-12, we see that $\frac{1}{2}mv^2 = kZe^2/2r$ (a result that holds for circular motion in any inverse-square force field), so the total energy can be written as

$$E = \frac{kZe^2}{2r} - \frac{kZe^2}{r} = -\frac{kZe^2}{2r} \sim -\frac{1}{r} \qquad \textbf{4-14}$$

Thus, classical physics predicts that, as energy is lost to radiation, the electron's orbit will become smaller and smaller while the frequency of the emitted radiation will become higher and higher, further increasing the rate at which energy is lost and ending when the electron reaches the nucleus. (See Figure 4-15*a*.) The time required for the electron to spiral into the nucleus can be calculated from classical mechanics and

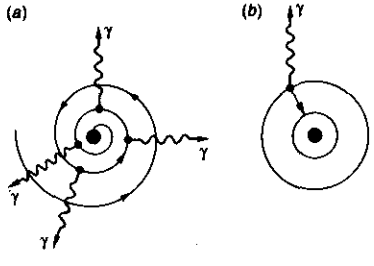

Fig. 4-15 (*a*) In the classical orbital model, the electron orbits about the nucleus and spirals into the center because of the energy radiated. (*b*) In the Bohr model, the electron orbits without radiating until it jumps to another allowed radius of lower energy, at which time radiation is emitted.

electrodynamics; it turns out to be less than a microsecond. Thus, at first sight, this model predicts that the atom will radiate a continuous spectrum (since the frequency of revolution changes continuously as the electron spirals in) and will collapse after a very short time, a result that fortunately does not occur. Unless excited by some external means, atoms do not radiate at all; and when excited atoms do radiate, a line spectrum is emitted, not a continuous one.

Bohr "solved" these formidable difficulties with two decidedly nonclassical postulates. His first postulate was that electrons could move in certain orbits without radiating. He called these orbits *stationary states*. His second postulate was to assume that the atom radiates when the electron makes a transition from one stationary state to another (Figure 4-15*b*) and that the frequency f of the emitted radiation is not the frequency of motion in either stable orbit but is related to the energies of the orbits by Planck's theory

$$hf = E_i - E_f \qquad \textbf{4-15}$$

where h is Planck's constant and E_i and E_f are the energies of the initial and final states. The second assumption, which is equivalent to that of energy conservation with the emission of a photon, is crucial because it deviated from classical theory, which requires the frequency of radiation to be that of the motion of the charged particle. Equation 4-15 is referred to as the Bohr *frequency condition*.

In order to determine the energies of the allowed, nonradiating orbits, Bohr made a third assumption, now known as the *correspondence principle*, which had profound implications:

> In the limit of large orbits and large energies, quantum calculations must agree with classical calculations.

Thus the correspondence principle says that, whatever modifications of classical physics are made to describe matter at the submicroscopic level, when the results are extended to the macroscopic world they must agree with those from the classical laws of physics that have been so abundantly verified in the everyday world. While Bohr's detailed model of the hydrogen atom has been supplanted by modern quantum theory, which we shall discuss in later chapters, his frequency condition (Equation 4-15) and the correspondence principle remain as essential features of the new theory.

In his first paper,[11] in 1913, Bohr pointed out that his results implied that the angular momentum of the electron in the hydrogen atom can take on only values that are integral multiples of Planck's constant divided by 2π, in agreement with a discovery made a year earlier by J. W. Nicholson. That is, angular momentum is quantized; it can assume only the values $nh/2\pi$, where n is an integer. Rather than follow the intricacies of Bohr's derivation, we shall use the fundamental conclusion of angular momentum quantization to find his expression for the observed spectra. The development that follows applies not only to hydrogen, but to any atom of nuclear charge $+Ze$ with a single orbital electron—e.g., singly ionized helium He^+, or doubly ionized lithium Li^{++}.

If the nuclear charge is $+Ze$ and the electron charge $-e$, we have noted (Equation 4-12) that the centripetal force necessary to move the electron in a circular orbit is provided by the Coulomb force kZe^2/r^2. Solving Equation 4-12 for the speed of the orbiting electron yields

$$v = \left(\frac{kZe^2}{mr}\right)^{1/2} \qquad \textbf{4-16}$$

Bohr's quantization of the angular momentum L is

$$L = mvr = \frac{nh}{2\pi} = n\hbar \qquad n = 1, 2, 3, \cdots \qquad \textbf{4-17}$$

where the integer n is called a *quantum number* and $\hbar = h/2\pi$. (The constant $\hbar$, read "h-bar," is often more convenient to use than h itself, just as the angular frequency $\omega = 2\pi f$ is often more convenient than the frequency f.) Combining Equations 4-16 and 4-17 allows us to write for the circular orbits:

$$r = \frac{n\hbar}{mv} = \frac{n\hbar}{m}\left(\frac{rm}{kZe^2}\right)^{1/2}$$

Squaring this relation gives

$$r^2 = \frac{n^2\hbar^2}{m^2}\left(\frac{rm}{kZe^2}\right)$$

and canceling common quantities yields

$$r_n = \frac{n^2\hbar^2}{mkZe^2} = \frac{n^2 a_0}{Z} \qquad \textbf{4-18}$$

where

$$a_0 = \frac{\hbar^2}{mke^2} = 0.529\text{Å} = 0.0529\text{ nm} \qquad \textbf{4-19}$$

is called the *Bohr radius*. Thus, we find that the stationary orbits of Bohr's first postulate have quantized radii, denoted in Equation 4-18 by the subscript on r_n. Notice that the Bohr radius a_0 for hydrogen ($Z = 1$) corresponds to the orbit radius with $n = 1$, the smallest Bohr orbit possible for the electron in a hydrogen atom. Since $r_n \sim Z^{-1}$, the Bohr orbits for single-electron atoms with $Z > 1$ are closer to the nucleus than the corresponding ones for hydrogen.

The total energy of the electron (Equation 4-14) then becomes, upon substitution of r_n from Equation 4-18,

$$E_n = -\frac{kZe^2}{2r_n} = -\frac{kZe^2}{2}\left(\frac{mkZe^2}{n^2\hbar^2}\right)$$

$$E_n = -\frac{mk^2Z^2e^4}{2\hbar^2n^2} = -E_0\frac{Z^2}{n^2} \qquad n = 1, 2, 3, \cdots \qquad \textbf{4-20}$$

where $E_0 = mk^2e^4/2\hbar^2$. Thus, the energy of the electron is also quantized, i.e., the stationary states correspond to specific values of the total energy. This means that energies E_i and E_f that appear in the frequency condition of Bohr's second postulate must be from the allowed set E_n and Equation 4-15 becomes

$$hf = E_{n_i} - E_{n_f} = -E_0\frac{Z^2}{n_i^2} - \left(-E_0\frac{Z^2}{n_f^2}\right)$$

or

$$f = \frac{E_0Z^2}{h}\left(\frac{1}{n_f^2} - \frac{1}{n_i^2}\right) \qquad \textbf{4-21}$$

which can be written in the form of the Rydberg-Ritz equation (Equation 4-2) by substituting $f = c/\lambda$ and dividing by c to obtain

$$\frac{1}{\lambda} = \frac{E_0Z^2}{hc}\left(\frac{1}{n_f^2} - \frac{1}{n_i^2}\right)$$

or

$$\frac{1}{\lambda} = Z^2R\left(\frac{1}{n_f^2} - \frac{1}{n_i^2}\right) \qquad \textbf{4-22}$$

where

$$R = \frac{E_0}{hc} = \frac{mk^2e^4}{4\pi c\hbar^3} \qquad \textbf{4-23}$$

is Bohr's prediction for the value of the Rydberg constant.

Using the values of m, e, c, and $\hbar$ known in 1913, Bohr calculated R and found his result to agree (within the limits of uncertainties of the constants) with the value obtained from spectroscopy, $1.097 \times 10^7\ \text{m}^{-1}$. Bohr noted in his original paper that this equation might be valuable in determining the best values for the constants e, m, and $\hbar$ because of the extreme precision possible in measuring R. This has indeed turned out to be the case.

The possible values of the energy of the hydrogen atom predicted by Bohr's model are given by Equation 4-20 with $Z = 1$:

$$E_n = -\frac{mk^2e^4}{2\hbar^2n^2} = -\frac{E_0}{n^2} \qquad \textbf{4-24}$$

where

$$E_0 = \frac{mk^2e^4}{2\hbar^2} = 2.18 \times 10^{-18}\text{ J} = 13.6\text{ eV}$$

is the magnitude of E_n with $n = 1$. E_1 ($= -E_0$) is called the *ground state*. It is convenient to plot these allowed energies of the stationary states as in Figure 4-16. Such a plot is called an *energy-level diagram*. Various series of transitions between the stationary states are indicated in this diagram by vertical arrows drawn between the levels. The frequency of light emitted in one of these transitions is the energy difference divided by h according to Bohr's frequency condition, Equation 4-15. The energy required to remove the electron from the atom, 13.6 eV, is called the *ionization energy*, or *binding energy*, of the electron.

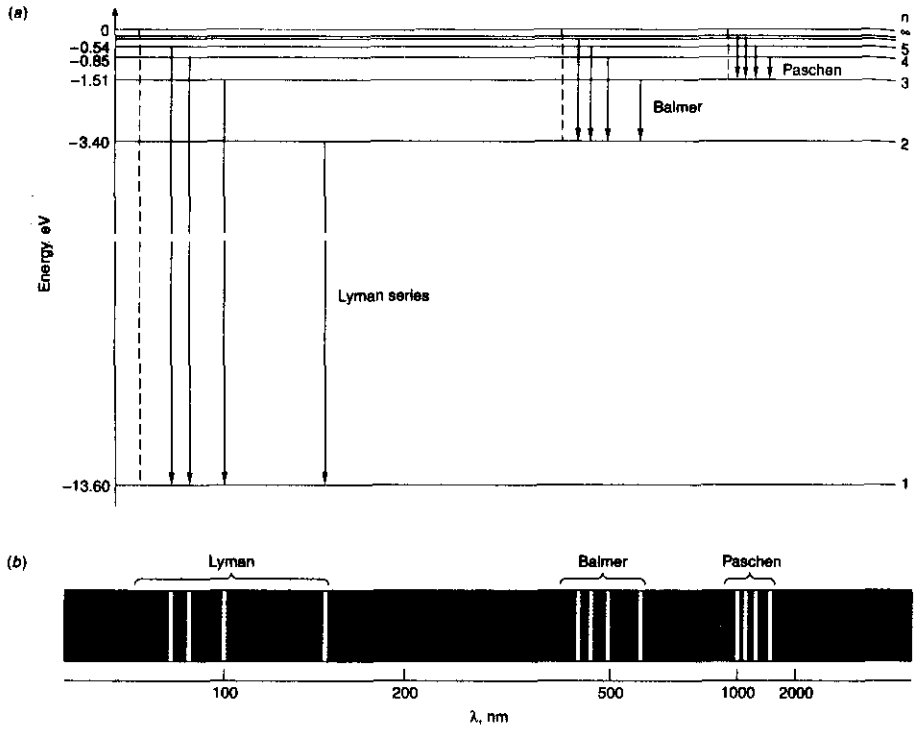

Fig. 4-16 (*a*) Energy-level diagram for hydrogen showing the seven lowest stationary states and the four lowest energy transitions each for the Lyman, Balmer, and Paschen series. There are an infinite number of levels. Their energies are given by $E_n = -13.6/n^2$ eV, where n is an integer. The dashed line shown for each series is the *series limit*, corresponding to the energy that would be radiated by an electron at rest far from the nucleus ($n \rightarrow \infty$) in a transition to the state with $n = n_f$ for that series. The horizontal spacing between the transitions shown for each series is proportional to the wavelength spacing between the lines of the spectrum. (*b*) The spectral lines corresponding to the transitions shown for the three series. Notice the regularities within each series, particularly the short-wavelength limit and the successively smaller separation between adjacent lines as the limit is approached. The wavelength scale in the diagram is not linear.

A bit different sort of application, the Bohr-Rutherford model of the nuclear atom and electron orbits is the picture that, for millions of people, provides their link to the world of the atom and subatomic phenomena.

At the time Bohr's paper was published there were two spectral series known for hydrogen: the Balmer series, corresponding to $n_f = 2$, $n_i = 3, 4, 5, \ldots$ and a series named after its discoverer, Paschen (1908), corresponding to $n_f = 3$, $n_i = 4, 5, 6, \ldots$. Equation 4-22 indicated that other series should exist for different values of n_f. In 1916 Lyman found the series corresponding to $n_f = 1$, and in 1922 and 1924 Brackett and Pfund, respectively, found series corresponding to $n_f = 4$ and $n_f = 5$. As can be easily determined by computing the wavelengths for these series, only the Balmer series lies primarily in the visible portion of the electromagnetic spectrum. The Lyman series is in the ultraviolet, the others in the infrared.

EXAMPLE 4-6 Wavelength of the H_β Line Compute the wavelength of the H_β spectral line, i.e., the second line of the Balmer series predicted by Bohr's model. The H_β line is emitted in the transition from $n_i = 4$ to $n_f = 2$.

Solution

1. *Method 1:* The wavelength is given by Equation 4-22 with $Z = 1$:

$$\frac{1}{\lambda} = R\left(\frac{1}{n_f^2} - \frac{1}{n_i^2}\right)$$

2. Substituting $R = 1.097 \times 10^7\ m^{-1}$ and the values of n_i and n_f:

$$\frac{1}{\lambda} = (1.097 \times 10^7)\left(\frac{1}{2^2} - \frac{1}{4^2}\right)$$

or

$$\lambda = 4.86 \times 10^{-7} = 486\ nm$$

3. *Method 2:* The wavelength may also be computed from Equation 4-15:

$$hf = hc/\lambda = E_i - E_f$$

or

$$\frac{1}{\lambda} = \frac{1}{hc}(E_i - E_f)$$

4. The values of E_i and E_f are given by Equation 4-24:

$$E_i = -\frac{13.6\ eV}{n_i^2} = -\frac{13.6\ eV}{4^2} = -0.85\ eV$$

$$E_f = -\frac{13.6\ eV}{n_f^2} = -\frac{13.6\ eV}{2^2} = -3.4\ eV$$

5. Substituting these into Equation 4-15 yields:

$$\frac{1}{\lambda} = \frac{[-0.85\ eV - (-3.4\ eV)](1.60 \times 10^{-19}\ J/eV)}{(6.63 \times 10^{-34}\ J \cdot s)(3.00 \times 10^8\ m/s)}$$
$$= 2.051 \times 10^6\ m^{-1}$$

or

$$\lambda = 4.87 \times 10^{-7}\ m = 487\ nm$$

Remarks: The difference in the two results is due to rounding of the Rydberg constant to three decimal places.

Reduced Mass Correction

The assumption by Bohr that the nucleus is fixed is equivalent to the assumption that it has infinite mass. In fact, the Rydberg constant in Equation 4-23 is normally written as R_∞, as we will do henceforth. If the nucleus has mass M its kinetic energy will be $\frac{1}{2}Mv^2 = p^2/2M$, where $p = Mv$ is the momentum. If we assume that the total momentum of the atom is zero, conservation of momentum requires that the momenta of the nucleus and electron be equal in magnitude. The total kinetic energy is then

$$E_k = \frac{p^2}{2M} + \frac{p^2}{2m} = \frac{M + m}{2mM}p^2 = \frac{p^2}{2\mu}$$

where

$$\mu = \frac{mM}{m + M} = \frac{m}{1 + m/M} \qquad \textbf{4-25}$$

This is slightly different from the kinetic energy of the electron because μ, called the *reduced mass*, is slightly different from the electron mass. The results derived above for a nucleus of infinite mass can be applied directly for the case of a nucleus of mass M if we replace the electron mass in the equations by reduced mass μ, defined by Equation 4-25. (The validity of this procedure is proven in most intermediate and advanced mechanics books.) The Rydberg constant (Equation 4-23) is then written

$$R = \frac{\mu k^2 e^4}{4\pi c\hbar^3} = \frac{mk^2e^4}{4\pi c\hbar^3}\left(\frac{1}{1 + m/M}\right) = R_\infty\left(\frac{1}{1 + m/M}\right) \qquad \textbf{4-26}$$

This correction amounts to only 1 part in 2000 for the case of hydrogen and to even less for other nuclei; however, the predicted variation in the Rydberg constant from atom to atom is precisely that which is observed. For example, the spectrum of a singly ionized helium atom, which has one remaining electron, is just that predicted by Equations 4-22 and 4-26 with $Z = 2$ and the proper helium mass. The current value for the Rydberg constant R_∞ from precision spectroscopic measurements[12] is

$$R_\infty = 1.0973731 \times 10^7\ \text{m}^{-1} \qquad \textbf{4-27}$$

Urey[13] used the reduced mass correction to the spectral lines of the Balmer series to discover (in 1931) a second form of hydrogen whose atoms had twice the mass of ordinary hydrogen. The heavy form was called *deuterium*. The two forms, atoms with the same Z but different masses, are called *isotopes*.

EXAMPLE 4-7 **Rydberg Constants for H and He$^+$** Compute the Rydberg constants for H and He$^+$ applying the reduced mass correction ($m = 9.1094 \times 10^{-31}$ kg, $m_p = 1.6726 \times 10^{-27}$ kg, $m_\alpha = 6.6447 \times 10^{-27}$ kg).

Solution

For hydrogen:

$$R_H = R_\infty\left(\frac{1}{1 + m/M_H}\right) = R_\infty\left(\frac{1}{1 + 9.1094 \times 10^{-31}/1.6726 \times 10^{-27}}\right)$$
$$= 1.09677 \times 10^7\ \text{m}^{-1}$$

For helium: Since M in the reduced mass correction is the mass of the nucleus, for this calculation we use M equal to the α particle mass.

$$R_{He} = R_\infty\left(\frac{1}{1 + 9.1094 \times 10^{-31}/6.6447 \times 10^{-27}}\right) = 1.09752 \times 10^7\ \text{m}^{-1}$$

Thus the two Rydberg constants differ by about 0.07 percent.

Correspondence Principle

According to the correspondence principle, which applies also to modern quantum mechanics, when the energy levels are closely spaced, quantization should have little effect; classical and quantum calculations should give the same results. From the energy-level diagram of Figure 4-16, we see that the energy levels are close together when the quantum number n is large. This leads us to a slightly different statement of Bohr's correspondence principle: in the region of very large quantum numbers (n in this case) classical calculation and quantum calculation must yield the same results. To see that the Bohr model of the hydrogen atom does indeed obey the correspondence principle, let us compare the frequency of a transition between level $n_i = n$ and level $n_f = n - 1$ for large n with the classical frequency, which is the frequency of revolution of the electron. From Equation 4-22 we have

$$f = \frac{c}{\lambda} = \frac{Z^2mk^2e^4}{4\pi\hbar^3}\left[\frac{1}{(n-1)^2} - \frac{1}{n^2}\right] = \frac{Z^2mk^2e^4}{4\pi\hbar^3}\frac{2n-1}{n^2(n-1)^2}$$

For large n we can neglect the 1s subtracted from n and $2n$ to obtain

$$f \approx \frac{Z^2mk^2e^4}{4\pi\hbar^3}\frac{2}{n^3} = \frac{Z^2mk^2e^4}{2\pi\hbar^3n^3} \qquad \textbf{4-28}$$

The classical frequency of revolution of the electron is (see Equation 4-13)

$$f_{rev} = \frac{v}{2\pi r}$$

Using $v = n\hbar/mr$ from Equation 4-17 and $r = n^2\hbar^2/mkZe^2$ from Equation 4-18, we obtain

$$f_{rev} = \frac{(n\hbar/mr)}{2\pi r} = \frac{n\hbar}{2\pi mr^2} = \frac{n\hbar}{2\pi m(n^2\hbar^2/mkZe^2)^2}$$
$$f_{rev} = \frac{m^2k^2Z^2e^4n\hbar}{2\pi mn^4\hbar^4} = \frac{mk^2Z^2e^4}{2\pi\hbar^3n^3} \qquad \textbf{4-29}$$

which is the same as Equation 4-28.

Fine-Structure Constant

The demonstration of the correspondence principle for large n in the preceding paragraph was for $\Delta n = n_i - n_f = 1$; however, we have seen (see Figure 4-16) that transitions occur in the hydrogen atom for $\Delta n \geq 1$ when n is small, and such transitions should occur for large n, too. If we allow $\Delta n = 2, 3, \ldots$ for large values of n, then the frequencies of the emitted radiation would be, according to Bohr's model, integer multiples of the frequency given in Equation 4-28. In that event, Equations 4-28 and 4-29 would not agree. This disagreement can be avoided by allowing elliptical orbits.[14] A result of Newtonian mechanics, familiar from planetary motion, is that in an inverse-square force field, the energy of an orbiting particle depends only on the major axis of the ellipse and not on its eccentricity. There is consequently no change in the energy at all unless the force differs from inverse square or unless Newtonian mechanics is modified. A. Sommerfeld considered the effect of special relativity on the mass of the electron in the Bohr model in an effort to explain the observed *fine structure* of the hydrogen spectral lines.[15] Since the relativistic corrections should be of the order of v^2/c^2 (see Chapter 2), it is likely that a highly eccentric orbit would have a larger correction, because v becomes greater as the electron moves nearer the nucleus. The Sommerfeld calculations are quite complicated, but we can estimate the order of magnitude of the effect of special relativity by calculating v/c for the first Bohr orbit in hydrogen. For $n = 1$, we have from Equation 4-17 that $mvr_1 = \hbar$. Then, using $r_1 = a_0 = \hbar^2/mke^2$, we have

$$v = \frac{\hbar}{mr_1} = \frac{\hbar}{m(\hbar^2/mke^2)} = \frac{ke^2}{\hbar}$$

and

$$\frac{v}{c} = \frac{ke^2}{\hbar c} = \frac{1.44\ \text{eV}\cdot\text{nm}}{197.3\ \text{eV}\cdot\text{nm}} \approx \frac{1}{137} = \alpha \qquad \textbf{4-30}$$

where we have used another convenient combination

$$\hbar c = \frac{1.24 \times 10^3\ \text{eV}\cdot\text{nm}}{2\pi} = 197.3\ \text{eV}\cdot\text{nm} \qquad \textbf{4-31}$$

The dimensionless quantity $ke^2/\hbar c = \alpha$ is called the *fine-structure constant* because of its first appearance in Sommerfeld's theory, but, as we shall see, it has much more fundamental importance.

Though v^2/c^2 is very small, an effect of this magnitude is observable. In Sommerfeld's theory, the fine structure of the hydrogen spectrum is explained in the following way. For each allowed circular orbit of radius r_n and energy E_n, a set of n elliptical orbits is possible of equal major axes but different eccentricities. Since the velocity of a particle in an elliptical orbit depends on the eccentricity, so then will the mass and momentum, and therefore the different ellipses for a given n will have slightly different energies. Thus, the energy radiated when the electron changes orbit depends slightly on the eccentricities of the initial and final orbits as well as on their major axes. The splitting of the energy levels for a given n is called *fine-structure splitting*, and its value turns out to be of the order of $v^2/c^2 = \alpha^2$, just as Sommerfeld predicted. However, the agreement of Sommerfeld's prediction with the observed fine-structure splitting was quite accidental and led to considerable confusion in the early days of quantum theory. Although he had used the relativistic mass and momentum, he computed the energy using classical mechanics, leading to a correction much larger than that actually due only to relativistic effects. As we shall see in Chapter 7, fine structure is associated with a completely nonclassical property of the electron called *spin*.

A lasting contribution of Sommerfeld's effort was the introduction of the fine-structure constant $\alpha = ke^2/\hbar c \approx 1/137$. With it we can write the Bohr radius a_0 and the quantized energies of the Bohr model in a particularly elegant form. Equations 4-24 and 4-19 for hydrogen become

$$E_n = -\frac{mk^2e^4}{2\hbar^2n^2} \cdot \frac{c^2}{c^2} = -\frac{mc^2}{2}\alpha^2\frac{1}{n^2} \qquad \textbf{4-32}$$

$$a_0 = \frac{\hbar^2}{mke^2} \cdot \frac{c}{c} = \frac{\hbar}{mc}\frac{1}{\alpha} \qquad \textbf{4-33}$$

Since α is a dimensionless number formed of universal constants, *all* observers will measure the same value for it and find that energies and dimensions of atomic systems are proportional to α^2 and $1/\alpha$, respectively. We will return to the implications of this intriguing fact later in the book.

Exploring *Giant Atoms*

Giant atoms called *Rydberg atoms*, long understood to be a theoretical possibility and first detected in interstellar space in 1965, are now being produced and studied in the laboratory. Notice in Equation 4-18 that the radius of the electron orbit $r_n \propto n^2$ and n can be any positive integer, so the diameter of a hydrogen atom (or any other atom, for that matter) could be very large, a millimeter or even a meter! What keeps such giant atoms from being common is that the energy difference between adjacent allowed energy states is extremely small when n is large and the allowed states are very near the $E_\infty = 0$ level where ionization occurs, because $E_n \propto 1/n^2$. For example, if $n = 1000$ the diameter of a hydrogen atom would be $r_{1000} \approx 0.1$ *mm*, but both E_{1000} and the difference in energy $\Delta E = E_{1001} - E_{1000}$ are about 10^{-5} eV! This energy is far below the average energy of thermal motion at ordinary temperatures (about 0.025 eV), so random collisions would quickly ionize an atom whose electron happened to get excited to a level with n equal to 20 or so with r still only about 10^{-6} m.

The advent of precisely tunable dye lasers in the 1970s made it possible to nudge electrons carefully into orbits with larger and larger n values. The largest Rydberg atoms made so far, typically using sodium or potassium, are 10,000 times the diameter of ordinary atoms, about 20 μm across or the size of a fine grain of sand, and exist for several milliseconds inside vacuum chambers. For hydrogen, this corresponds to quantum number $n \approx 600$. An electron moving so far from the nucleus is bound by a minuscule force. This provides several intriguing possibilities. For example, very small electric fields might be studied, enabling the tracking of chemical reactions that proceed too quickly to be followed otherwise. More dramatic is the possibility of directly testing Bohr's correspondence principle by directly observing the slow (since $v \propto 1/n$) movement of the electron around the

large n orbits—the transition from quantum mechanics to classical mechanics. Computer simulations of the classical motion of a Rydberg electron "wave" (see Chapter 5) in orbit around a nucleus are aiding in the design of experiments to observe the correspondence principle.

QUESTIONS

6. If the electron moves in an orbit of greater radius, does its total energy increase or decrease? Does its kinetic energy increase or decrease?
7. What is the energy of the shortest-wavelength photon that can be emitted by the hydrogen atom?
8. How would you characterize the motion and location of an electron with $E = 0$ and $n \rightarrow \infty$ in Figure 4-16?

4-4 X-Ray Spectra

Henry G.-J. Moseley. [*Courtesy of University of Manchester.*]

The extension of the Bohr theory to atoms more complicated than hydrogen proved difficult. Quantitative calculations of the energy levels of atoms of more than one electron could not be made from the model, even for helium, the next element in the periodic table. However, experiments by H. Moseley in 1913 and J. Franck and G. Hertz in 1914 strongly supported the general Bohr-Rutherford picture of the atom as a positively charged core surrounded by electrons that moved in quantized energy states relatively far from the core. Moseley's analysis of x-ray spectra will be discussed in this section, and the Franck-Hertz measurement of the transmission of electrons through gases will be discussed in the next section.

Using the methods of crystal spectrometry that had just been developed by W. H. Bragg and W. L. Bragg, Moseley[16] measured the wavelengths of the characteristic x-ray line spectra for about 40 different target elements. (Typical x-ray spectra were shown in Figure 3-18.) He noted that the x-ray line spectra varied in a regular way from element to element, unlike the irregular variations of optical spectra. He surmised that this regular variation occurred because characteristic x-ray spectra were due to transitions involving the innermost electrons of the atoms. (see Figure 4-17.) Because the inner electrons are shielded from the outermost electrons by those in intermediate orbits, their energies do not depend on the complex interactions of the outer electrons, which are responsible for the complicated optical spectra. Furthermore, the inner electrons are well shielded from the interatomic forces which are responsible for the binding of atoms in solids.

According to the Bohr theory (published earlier the same year, 1913), the energy of an electron in the first Bohr orbit is proportional to the square of the nuclear charge (see Equation 4-20). Moseley reasoned that the energy, and therefore the frequency, of a characteristic x-ray photon should vary as the square of the atomic number of the target element. He therefore plotted the square root of the frequency of a particular characteristic line in the x-ray spectrum of various target elements versus the atomic number Z of the element. Such a plot, now called a *Moseley plot*, is shown in Figure 4-18 (page 188). These curves can be fitted by the empirical equation

$$f^{1/2} = A_n(Z - b) \qquad \textbf{4-34}$$

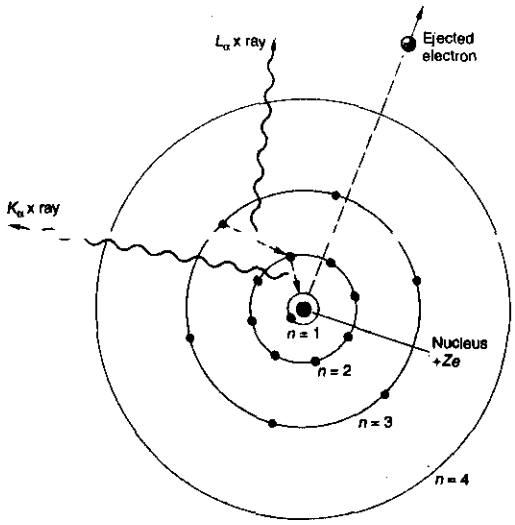

Fig. 4-17 A stylized picture of the Bohr circular orbits for $n = 1, 2, 3$, and 4. The radii $r_n \sim n^2$. In a high-Z element (elements with $Z \geq 12$ emit x rays), electrons are distributed over all the orbits shown. Should an electron in the $n = 1$ orbit be knocked from the atom, e.g., by being hit by a fast electron accelerated by the voltage across an x-ray tube, the vacancy thus produced is filled by an electron of higher energy (i.e., $n = 2$ or higher). The difference in energy between the two orbits is emitted as a photon, according to the frequency condition, whose wavelength will be in the x-ray region of the spectrum, if Z is large enough.

where A_n and b are constants for each characteristic x-ray line. One family of lines, called the *K series*, has $b = 1$ and slightly different values of A_n for each line in the graph. The other family shown in Figure 4-18, called the *L series*,[17] could be fitted by Equation 4-34 with $b = 7.4$.

If the bombarding electron in the x-ray tube knocks an electron from the inner orbit ($n = 1$) in a target atom completely out of the atom, photons will be emitted corresponding to transitions of electrons in other orbits ($n = 2, 3, \ldots$) to fill the vacancy in the $n = 1$ orbit. (See Figure 4-17.) (Since these lines are called the *K series*, the $n = 1$ orbit came to be called the *K shell*.) The lowest-frequency line corresponds to the lowest energy transition ($n = 2$ to $n = 1$). This line is called the K_α line. The transition $n = 3$ to $n = 1$ is called the K_β line. It is of higher energy, and hence higher frequency, than the K_α line. A vacancy created in the $n = 2$ orbit by emission of a K_α x ray may then be filled by an electron of higher energy, e.g., one in the $n = 3$ orbit, resulting in the emission of a line in the L series, and so on. The multiple L lines in the Moseley plot (Figure 4-18) are due in part to the fact that there turn out to be small differences in the energies of electrons with a given n that are not predicated by the Bohr model. Moseley's work gave the first indication of these differences, but the explanation will have to await our discussion of more advanced quantum theory in Chapter 7.

Using the Bohr relation for a one-electron atom (Equation 4-21) with $n_f = 1$, and using $(Z - 1)$ in place of Z, we obtain for the frequencies of the K series

$$f = \frac{mk^2e^4}{4\pi\hbar^3}(Z - 1)^2\left(\frac{1}{1^2} - \frac{1}{n^2}\right) = cR_\infty(Z - 1)^2\left(1 - \frac{1}{n^2}\right) \qquad \textbf{4-35}$$

where R_∞ is the Rydberg constant. Comparing this with Equation 4-34, we see that A_n is given by

$$A_n^2 = cR_\infty\left(1 - \frac{1}{n^2}\right) \qquad \textbf{4-36}$$

The wavelengths of the lines in the K series are then given by

$$\lambda = \frac{c}{f} = \frac{c}{A_n^2(Z-1)^2} = \frac{1}{R_\infty(Z-1)^2\left(1 - \frac{1}{n^2}\right)} \qquad \textbf{4-37}$$

EXAMPLE 4-8 K_α for Molybdenum Calculate the wavelength of the K_α line of molybdenum ($Z = 42$), and compare the result with the value $\lambda = 0.0721$ nm measured by Moseley and with the spectrum in Figure 3-18*b*.

Solution
Using $n = 2$, $R_\infty = 1.097 \times 10^7\ \text{m}^{-1}$, and $Z = 42$ we obtain

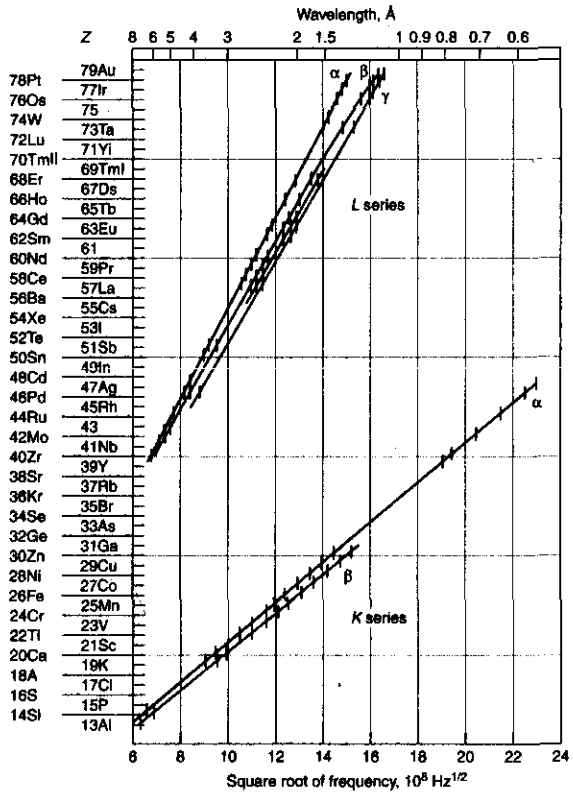

Fig. 4-18 Moseley's plots of the square root of frequency versus Z for characteristic x rays. When an atom is bombarded by high-energy electrons, an inner atomic electron is sometimes knocked out, leaving a vacancy in the inner shell. The K-series x rays are produced by atomic transitions to vacancies in the $n = 1$ (K) shell, whereas the L series is produced by transitions to the vacancies in the $n = 2$ (L) shell. [*From H. Moseley,* Philosophical Magazine *(6), 27, 713 (1914).*]

$$\lambda = \left[(1.097 \times 10^7\ \text{m}^{-1})(41)^2\left(1 - \frac{1}{4}\right)\right]^{-1} = 7.23 \times 10^{-11}\ \text{m} = 0.0723\ \text{nm}$$

This value is within 0.3 percent of Moseley's measurement and agrees well with that in Figure 3-18*b*.

The fact that f is proportional to $(Z-1)^2$ rather than to Z^2 is explained by the partial shielding of the nuclear charge by the other electron remaining in the K shell [illegible] cluded that, since $b = 7.4$ for the L series, these lines involved electrons farther from the nucleus, which "saw" the nuclear charge shielded by more inner electrons. Assuming that the L series was due to transitions to the $n = 2$ shell, the frequencies for this series are given by

$$f = cR_\infty\left(\frac{1}{2^2} - \frac{1}{n^2}\right)(Z - 7.4)^2 \qquad \textbf{4-38}$$

where $n = 3, 4, 5, \ldots$.

Before Moseley's work, the atomic number was merely the place number of the element in Mendeleev's periodic table of the element arranged by weight. The experiments of Geiger and Marsden showed that the nuclear charge was approximately $A/2$, while x-ray scattering experiments by Barkla showed that the number of electrons in an atom was approximately $A/2$. These two experiments are consistent, since the atom as a whole must be electrically neutral. However, several discrepancies were found in the periodic table as arranged by weight. For example, the 18th element in order of weight is potassium (39.102), and the 19th is argon (39.948). Arrangement by weight, however, puts potassium in the column with the inert gases and argon with the active metals, the reverse of their known chemical properties.

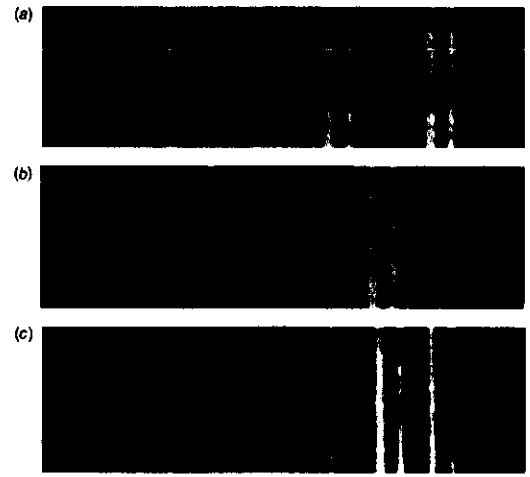

Fig. 4-19 Characteristic x-ray spectra. (*a*) Part of the spectra of neodymium ($Z = 60$) and samarium ($Z = 62$). The two pairs of bright lines are the K_α and K_β lines. (*b*) Part of the spectrum of the artificially produced element promethium ($Z = 61$). This element was first positively identified in 1945 at the Clinton Laboratory (now Oak Ridge). Its K_α and K_β lines fall between those of neodymium and samarium, just as Moseley predicted. (*c*) Part of the spectra of all three of the elements neodymium, promethium, and samarium. [*Courtesy of J. A. Swartout, Oak Ridge National Laboratory.*]

Moseley showed that for these elements to fall on the line $f^{1/2}$ versus Z, argon had to have $Z = 18$ and potassium $Z = 19$. Arranging the elements by the Z number obtained from the Moseley plot, rather than by weight, gave a periodic chart in complete agreement with the chemical properties. Moseley also pointed out that there were gaps in the periodic table at $Z = 43$, 61, and 75, indicating the presence of undiscovered elements. All have subsequently been found. Figure 4-19 illustrates the discovery of promethium ($Z = 61$).

Auger Electrons

The process of producing x rays necessarily results in the ionization of the atom, since an inner electron is ejected. The vacancy created is filled by an outer electron, producing the x rays studied by Moseley. In 1923 Pierre Auger discovered that, as an alternative to x-ray emission, the atom may eject a third electron from a higher-energy outer shell via a radiationless process called the *Auger effect*. In the Auger (pronounced "oh-zhay") process, the energy difference $\Delta E = E_2 - E_1$ that could have resulted in the emission of a K_α x ray is removed from the atom by the third

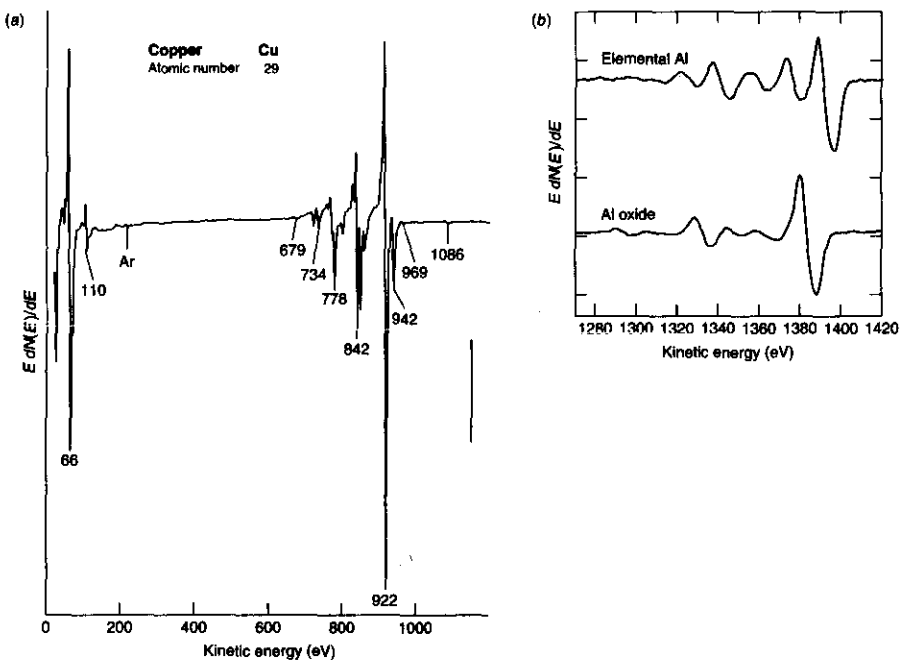

Fig. 4-20 (*a*) The Auger spectrum of Cu bombarded with 10-keV electrons. The energy of the Auger electrons is more precisely determined by plotting the weighted derivative $E\,dN(E)/dE$ of the electron intensity rather than the intensity $N(E)$. (*b*) A portion of the Auger spectrum of Al from elemental Al and Al oxide. Note the energy shift in the largest peaks resulting from adjustments in the Al electron shell energies in the Al_2O_3 molecule.

electron, e.g., one in the $n = 3$ shell. Since the magnitude of $E_3 < \Delta E$, the $n = 3$ electron would leave the atom with a characteristic kinetic energy $\Delta E - |E_3|$, which is determined by the stationary-state energies of the particular atom.[19] Thus, each element has a characteristic Auger electron spectrum. (See Figure 4-20*a*.) Measurement of the Auger electrons provides a simple and highly sensitive tool for identifying impurities on clean surfaces in electron microscope systems and investigating electron energy shifts associated with molecular bonding. (See Figure 4-20*b*.)

9. Why did Moseley plot $f^{1/2}$ versus Z rather than f versus Z?

4-5 The Franck-Hertz Experiment

While investigating the inelastic scattering of electrons, J. Franck and G. Hertz[20] performed an important experiment that confirmed by direct measurement Bohr's hypothesis of energy quantization in atoms. First done in 1914, it is now a standard undergraduate laboratory experiment. Figure 4-21*a* is a schematic diagram of the apparatus. A small heater heats the cathode. Electrons are ejected from the heated cathode and accelerated toward a grid, which is at a positive potential V_0 relative to the cathode. Some electrons pass through the grid and reach the plate P, which is at a slightly lower potential $V_p = V_0 - \Delta V$. The tube is filled with a low-pressure gas of the element

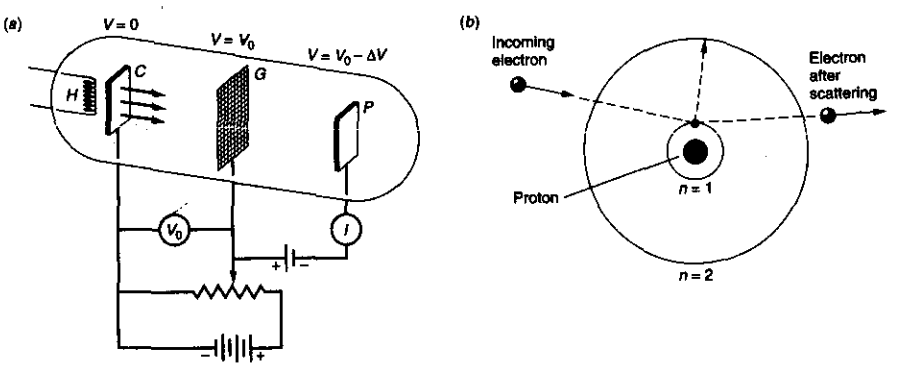

Fig. 4-21 (*a*) Schematic diagram of the Franck-Hertz experiment. Electrons ejected from the heated cathode C at zero potential are drawn to the positive grid G. Those passing through the holes in the grid can reach the plate P and thereby contribute to the current I, if they have sufficient kinetic energy to overcome the small back potential ΔV. The tube contains a low-pressure gas of the element being studied. (*b*) Results for hydrogen. If the incoming electron does not have sufficient energy to transfer $\Delta E = E_2 - E_1$ to the hydrogen electron in the $n = 1$ orbit (ground state), then the scattering will be elastic. If the incoming electron does have at least ΔE kinetic energy, then an inelastic collision can occur in which ΔE is transferred to the $n = 1$ electron, moving it to the $n = 2$ orbit. The excited electron will typically return to the ground state very quickly, emitting a photon of energy ΔE.

being investigated (mercury vapor, in Franck and Hertz's experiment). The experiment involves measuring the plate current as a function of V_0. As V_0 is increased from 0, the current increases until a critical value (about 4.9 V for Hg) is reached, at which point the current suddenly decreases. As V_0 is increased further, the current rises again.

The explanation of this result is a bit easier to visualize if we think for the moment of a tube filled with hydrogen atoms instead of mercury. (See Figure 4-21*b*.) Electrons accelerated by V_0 that collide with hydrogen electrons cannot transfer energy to the latter unless they have acquired kinetic energy $eV_0 = E_2 - E_1 = 10.2$ eV, since the hydrogen electron according to Bohr's model cannot occupy states with energies intermediate between E_1 and E_2. Such a collision will thus be elastic; i.e., the incident electron's kinetic energy will be unchanged by the collision, and thus it can overcome the small retarding potential ΔV and contribute to the current I. However, if $eV_0 \geq 10.2$ eV, then the incoming electron can transfer 10.2 eV to the hydrogen electron in the *ground state* ($n = 1$ orbit), putting it into the $n = 2$ orbit (the *first excited state*). The incoming electron's energy is thus reduced by 10.2 eV; it has been inelastically scattered. With insufficient energy to overcome the small retarding potential ΔV, the incoming electrons can no longer contribute to the plate current I, and I drops sharply.

The situation with Hg in the tube is more complicated, since Hg has 80 electrons. Although Bohr's theory is not capable of predicting their individual energies, we still expect the energy to be quantized with a ground state, first excited state, and so on, for the atom. Thus, the explanation of the observed 4.9-V critical potential for Hg is that the first excited state is about 4.9 eV above the lowest level (ground state). Electrons with energy less than this cannot lose energy to the Hg atoms, but electrons with energy greater than 4.9 eV can make inelastic collisions and lose 4.9 eV. If this happens near the grid, these electrons cannot gain enough energy to overcome the small back voltage ΔV and reach the plate; the current therefore decreases. If this explanation is correct, the Hg atoms that are excited to an energy level of 4.9 eV above the ground state should return to the ground state by emitting light of wavelength

$$\lambda = \frac{c}{f} = \frac{hc}{hf} = \frac{hc}{eV_0} = 253 \text{ nm}$$

There is indeed a line of this wavelength in the mercury spectrum. When the tube is viewed with a spectroscope, this line is seen when V_0 is greater than 4.9 eV, while no lines are seen when V_0 is less than this amount. For further increases in V_0, additional sharp decreases in the current are observed, corresponding either to excitation of other levels in Hg (e.g., the second excited state of Hg is at 6.7 eV above the ground state) or to multiple excitation of the first excited state, i.e., due to an electron losing 4.9 eV more than once. In the usual setup, multiple excitations of the first level are observed and decreases in the current are seen at integer multiples of 4.9 eV.[21] The probability of observing such multiple first-level excitations, or excitations of other levels, depends on the detailed variation of the potential of the tube. For example, a second decrease in the current at $V_0 = 2 \times 4.9 = 9.8$ V results when electrons have inelastic collisions with Hg atoms about halfway between the cathode and grid (see Figure 4-21*a*). They are reaccelerated, reaching 4.9 eV again in the vicinity of the grid. A plot of the data of Franck and Hertz is shown in Figure 4-22.

The Franck-Hertz experiment was an important confirmation of the idea that discrete optical spectra were due to the existence in atoms of discrete energy levels which could be excited by nonoptical methods. It is particularly gratifying to be able to detect the existence of discrete energy levels directly by measurements using only voltmeters and ammeters.

Electron Energy Loss Spectroscopy

The Franck-Hertz experiment was the precursor of a highly sensitive technique for measuring the quantized energy states of atoms in both gases and solids. The technique, called *electron energy loss spectroscopy* (*EELS*), is particularly useful in solids, where it makes possible measurement of the energy of certain types of lattice vibrations and other processes. It works like this. Suppose that the electrons in an incident beam all have energy E_{inc}. They collide with the atoms of a material, causing them to undergo some process (e.g., vibration, lattice rearrangement, electron excitation) that requires energy E_1. Then, if a beam electron initiates a single such process, it will exit the material with energy $E_{inc} - E_1$—i.e., it has been inelastically scattered. The exit energy can be measured very accurately with, e.g., a magnetic spectrometer similar to that described in Section 3-1, but designed for electrons.[22] Figure 4-23*a* illustrates a typical experimental arrangement for measuring an energy-loss spectrum.

As an example of its application, if an incident beam of electrons with $E_{inc} = 2$ keV is reflected from a thin Al film, the scattered electron energies measured in the magnetic spectrometer result in the energy-loss spectrum shown in Figure 4-23*b*, which directly represents the quantized energy levels of the target material. The loss peaks in this particular spectrum are due to the excitation of harmonic vibrations in the film, as well as some surface vibrations. The technique is also used to measure the vibrational energies of impurity atoms that may be absorbed on the surface and, with higher incident electron energies, to measure energy losses at the atomic inner levels, thus yielding information about bonding and other characteristics of absorbed atoms. Inelastic scattering techniques, including those using particles in addition to electrons, provide very powerful means for probing the energy structure of atomic, molecular, and nuclear systems. We will have occasion to refer to them many times throughout the rest of the book.

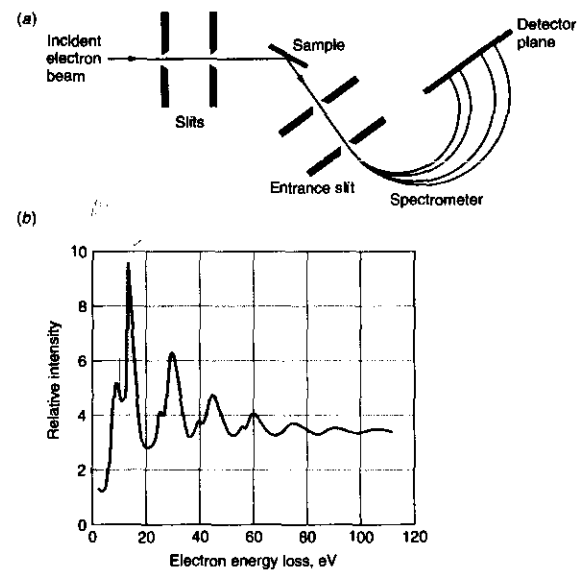

Fig. 4-23 Energy-loss spectrum measurement. (*a*) A well-defined electron beam impinges upon the sample. Electrons inelastically scattered at a convenient angle enter the slit of the magnetic spectrometer, whose B field is directed out of the paper, and turn through radii R determined by their energy ($E_{inc} - E_1$) via Equation 3-2 written in the form $R = [2m(E_{inc} - E_1)]^{1/2}/eB$. (*b*) An energy-loss spectrum for a thin Al film. [*From C. J. Powell and J. B. Swan,* Physical Review, *115, 869 (1954).*]

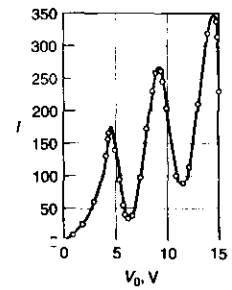

Fig. 4-22 Current versus accelerating voltage in the Franck-Hertz experiment. The current decreases because many electrons lose energy due to inelastic collisions with mercury atoms in the tube and therefore cannot overcome the small back potential indicated in Figure 4-21*a*. The regular spacing of the peaks in this curve indicates that only a certain quantity of energy, 4.9 eV, can be lost to the mercury atoms. This interpretation is confirmed by the observation of radiation of photon energy 4.9 eV emitted by the mercury atoms, when V_0 is greater than 4.9 V. [*From J. Franck and G. Hertz,* Verband Deutscher Physiklischer Gesellschaften, *16, 457 (1914).*]

4-6 Critique of Bohr Theory and of the "Old" Quantum Mechanics

We have seen in this and the preceding chapters that many phenomena—blackbody radiation, the photoelectric effect, Compton scattering, optical spectra of hydrogen, and the x-ray spectra of many elements—could be "explained" by various ad hoc quantum assumptions. These "theories," a strange mixture of classical physics and quantum assumptions, are now usually referred to as "old" quantum mechanics. Applying this quantum mechanics in the early years of the twentieth century was as much an art as a science, for no one knew exactly what the rules were. The successes of the Bohr theory, however, were substantial and spectacular. The existence of unknown spectral lines was predicted and later observed. Not only was the Rydberg constant given in terms of known constants, but its slight variation from atom to atom was accurately predicted by the slight variation in the reduced mass. The radius of the first Bohr orbit in hydrogen, 0.053 nm, corresponded well with the known diameter of the hydrogen molecule, about 0.22 nm. The wavelengths of the characteristic x-ray spectra could be calculated from the Bohr theory.

The failures of the Bohr theory and the old quantum mechanics were mainly matters of omission. While the correct H atom transitions were predicted, the theory was silent on the *rate* at which they occurred; i.e., there was no way of predicting the relative intensities of spectral lines. There was little success in applying the theory to the optical spectra of more complex atoms. Finally, there was the considerable philosophical problem that its assumptions lacked foundation. There were no a priori reasons to expect that Coulomb's law would work but that the laws of radiation would not, or that Newton's laws could be used even though only certain values of angular momentum were allowed. In the 1920s scientists struggled with these difficulties, and a systematic theory, now known as *quantum mechanics* or *wave mechanics*, was formulated by de Broglie, Schrödinger, Heisenberg, Pauli, Dirac, and others. We shall study some aspects of this theory in the next two chapters and apply it to the study of atoms, nuclei, and solids in the remaining chapters of this book. We shall see that, though this theory is much more satisfying from a philosophical point of view, it is somewhat abstract and difficult to apply in detail to problems. In spite of its shortcomings, the Bohr theory provides a model that is easy to visualize, gives the correct energy levels in hydrogen, and is often useful in describing a quantum-mechanical calculation.

Summary

TOPIC	RELEVANT EQUATIONS AND REMARKS	
1. Atomic spectra	$\frac{1}{\lambda_{nm}} = R\left(\frac{1}{m^2} - \frac{1}{n^2}\right) \quad n > m$	4-2
	This empirical equation computes the correct wavelengths of observed spectral lines. The Rydberg constant R varies in a regular way from element to element.	
2. Rutherford scattering		
Impact parameter	$b = \frac{kq_\alpha Q}{m_\alpha v^2}\cot\frac{\theta}{2}$	4-3
Scattered fraction f	$f = \pi b^2 nt$	4-5
	for a scattering foil with n nuclei/unit volume and thickness t	
Number of scattered alphas observed	$\Delta N = \left(\frac{I_0 A_{sc} nt}{r^2}\right)\left(\frac{kZe^2}{2E_k}\right)^2 \frac{1}{\sin^4(\theta/2)}$	4-6
[illegible]	$\frac{kq_\alpha Q}{\frac{1}{2}m_\alpha v^2}$	4-11
3. Bohr model		
Bohr's postulates	1. Electrons occupy only certain nonradiating, stable, circular orbits selected by quantization of the angular momentum L.	
	$L = mvr = \frac{nh}{2\pi} = n\hbar$ for integer n	4-17
	2. Radiation of frequency f occurs when the electron jumps from an allowed orbit of energy E_i to one of lower energy E_f. f is given by the frequency condition:	
	$hf = E_i - E_f$	4-15
Correspondence principle	In the region of very large quantum numbers classical and quantum calculations must yield the same results.	
Bohr radius	$a_0 = \frac{\hbar^2}{mke^2} = \frac{\hbar}{mc\alpha} = 0.0529\text{ nm}$	4-19
Allowed energies	$E_n = -\frac{Z^2 E_0}{n^2}$ for $n = 1, 2, 3, \ldots$	4-20
	where $E_0 = mk^2e^4/2\hbar^2 = 13.6\text{ eV}$	
Reduced mass	$\mu = \frac{mM}{m + M}$	4-25
Fine-structure constant	$\alpha = \frac{ke^2}{\hbar c} \approx 1/137$	4-30
4. X-ray spectra		
Moseley equation	$f^{1/2} = A_n(Z - b)$	4-34
5. Franck-Hertz experiment	Supported Bohr's theory by verifying the quantization of atomic energies in absorption.	

General References

The following general references are written at a level appropriate for the readers of this book.

Boorse, H., and L. Motz (eds.), *The World of the Atom*, Basic Books, New York, 1966. This two-volume, 1873-page work is a collection of original papers, translated and edited. Much of the work referred to in this chapter and throughout this book can be found in these volumes.

Cline, B., *The Questioners: Physicists and the Quantum Theory*, Thomas Y. Crowell, New York, 1965.

Gamow, G., *Thirty Years That Shook Physics: The Story of the Quantum Theory*, Doubleday, Garden City, N.Y., 1965.

Herzberg, G., *Atomic Spectra and Atomic Structure*, Dover, New York, 1944. This is without doubt one of the all-time classics of atomic physics.

Melissinos, A., *Experiments in Modern Physics*, Academic Press, New York, 1966. Many of the classic experiments that are now undergraduate laboratory experiments are described in detail in this text.

Mohr, P. J., and B. N. Taylor, "The Fundamental Physical Constants," *Physics Today* (August 2002).

Shamos, M. H. (ed.), *Great Experiments in Physics*, Holt, Rinehart & Winston, New York, 1962.

Virtual Laboratory (PEARL), Physics Academic Software, North Carolina State University, Raleigh, 1996. Includes an interactive model of the Bohr atom.

Visual Quantum Mechanics, Kansas State University, Manhattan, 1996. The atomic spectra component of this software provides an interactive construction of the energy levels for several elements, including hydrogen and helium.

Notes

1. Joseph von Fraunhofer (1787–1826), German physicist. Although he was not the first to see the dark lines in the solar spectrum that bear his name (Wollaston had seen seven, 12 years earlier), he systematically measured their wavelengths, named the prominent ones, and showed that they always occurred at the same wavelength, even if the sunlight were reflected from the moon or a planet.

2. To date more than 10,000 Fraunhofer lines have been found in the solar spectrum.

3. Although experimentalists preferred to express their measurements in terms of wavelengths, it had been shown that the many empirical formulas being constructed to explain the observed regularities in the line spectra could be expressed in simpler form if the reciprocal wavelength, called the *wave number* and equal to the number of waves per unit length, were used instead. Since $c = f\lambda$, this was equivalent to expressing the formulas in terms of the frequency.

4. Ernest Rutherford (1871–1937), English physicist, an exceptional experimentalist and a student of J. J. Thomson. He was an early researcher in the field of radioactivity and received the Nobel Prize in 1908 for his work in the transmutation of elements. He bemoaned the fact that his prize was awarded in chemistry, not in physics, as work with the elements was considered chemistry in those days. He was Thomson's successor as director of the Cavendish Laboratory.

5. Alpha particles, like all charged particles, lose energy by exciting and ionizing the molecules of the materials through which they are moving. The energy lost per unit path length ($-dE/dx$) is a function of the ionization potential of the molecules, the atomic number of the atoms, and the energy of the α particles. It can be computed (with some effort) and is relatively simple to measure experimentally.

6. Notice that $2\pi \sin\theta\, d\theta = d\Omega$, the differential solid angle subtended at the scattering nucleus by the surface in Figure 4-11. Since the cross section $\sigma = \pi b^2$, then $d\sigma = 2\pi b\, db$ and Equation 4-9 can be rewritten as

$$\frac{d\sigma}{d\Omega} = \left(\frac{kZe^2}{m_\alpha v^2}\right)^2 \frac{1}{\sin^4(\theta/2)}$$

$d\sigma/d\Omega$ is called the *differential cross section.*

7. H. Geiger and E. Marsden, *Philosophical Magazine* (6), **25**, 605 (1913).

8. The value of Z could not be measured directly in this experiment; however, relative values for different foil materials could be found and all materials heavier than aluminum had Z approximately equal to half the atomic weight.

9. This also introduces a deviation from the predicted ΔN associated with Rutherford's assumption that the nuclear mass was much larger than the α particle mass. For lighter-atomic-weight elements that assumption is not valid. Correction for the nuclear mass effect can be made, however, and the data in Figure 4-12*b* reflect the correction.

10. Niels H. D. Bohr (1885–1962), Danish physicist and first-rate soccer player. He went to the Cavendish Laboratory to work with J. J. Thomson after receiving his Ph.D.; however, Thomson is reported to have been impatient with Bohr's soft, accented English. Happily, the occasion of Thomson's annual birthday banquet brought Bohr in contact with Rutherford, whom he promptly followed to the latter's laboratory at Manchester, where he learned of the nuclear atom. A giant of twentieth-century physics, Bohr was awarded the Nobel Prize in 1922 for his explanation of the hydrogen spectrum. On a visit to the United States in 1939, he brought the news that the fission of uranium atoms had been observed. The story of his life makes absolutely fascinating reading.

11. N. Bohr, *Philosophical Magazine* (6), **26**, 1 (1913).

12. P. J. Mohr and B. N. Taylor, "The Fundamental Physical Constants," *Physics Today* (August 2002). Only 8 of the 14 current significant figures are given in Equation 4-27. The relative uncertainty in the value is about 1 part in 10^{12}!

13. Harold C. Urey (1893–1981), American chemist. His work opened the way for the use of isotopic tracers in biological systems. He was recognized with the Nobel Prize in 1934.

14. The basic reason that elliptical orbits solve this problem is that the frequency of the radiation emitted classically depends on the acceleration of the charge. The acceleration is constant for a circular orbit, but varies for elliptical orbits, being dependent on the instantaneous distance from the focus. The energy of a particle in a circular orbit of radius r is the same as that of a particle in an elliptical orbit with a semimajor axis of r, so one would expect the only allowed elliptical orbits to be those whose semimajor axis was equal to an allowed Bohr circular orbit radius.

15. Viewed with spectrographs of high resolution, the spectral lines of hydrogen in Figure 4-2*a*—and, indeed, most spectral lines of all elements—are found to consist of very closely spaced sets of lines, i.e., fine structure. We will discuss this topic in detail in Chapter 7.

16. Henry G.-J. Moseley (1887–1915), English physicist, considered by some the most brilliant of Rutherford's students. He would surely have been awarded the Nobel Prize had he not been killed in action in World War I. His father was a naturalist on the expedition of HMS *Challenger*, the first vessel ever devoted to the exploration of the oceans.

17. The identifiers L and K were assigned by the English physicist C. G. Barkla, the discoverer of the characteristic x-ray lines, for which he received the Nobel Prize in 1917. He discovered two sets of x-ray lines for each of several elements, the *longer* wavelength of which he called the L series, the other the K series. The identifiers stuck and were subsequently used to label the atomic electron shells.

18. That the remaining K electron should result in $b = 1$, i.e., shielding of exactly 1*e*, is perhaps a surprise. Actually it was a happy accident. It is the combined effect of the remaining K electron and the penetration of the electron waves of the outer L electrons that resulted in making $b = 1$, as we will see in Chapter 7.

19. Since in multielectron atoms the energies of the stationary states depend in part on the number of electrons in the atom (see Chapter 7), the energies E_n for a given atom change slightly when it is singly ionized, as in the production of characteristic x-ray lines, or doubly ionized, as in the Auger effect.

20. James Franck (1882–1964), German-American physicist; Gustav L. Hertz (1887–1975), German physicist. Franck won an Iron Cross as a soldier in World War I and later worked on the Manhattan Project. Hertz was a nephew of Heinrich Hertz, discoverer of the photoelectric effect. For their work on the inelastic scattering of electrons, Franck and Hertz shared the 1925 Nobel Prize in physics.

21. We should note at this point that there is an energy state in the Hg atom at about 4.6 eV, slightly lower than the one found by Franck and Hertz. However, transitions from the ground state to the 4.6-eV level are not observed, and their absence is in accord with the prediction of more advanced quantum mechanics, as we shall see in Chapter 7.

22. Since q/m for electrons is much larger than for ionized atoms, the radius for an electron magnetic spectrometer need not be as large as for a mass spectrometer, even for electron energies of several keV. (See Equation 3-2.)

Problems

Level 1

Section 4-1 Atomic Spectra

4-1. Compute the wavelength and frequency of the series limit for the Lyman, Balmer, and Paschen spectral series of hydrogen.

4-2. The wavelength of a particular line in the Balmer series is measured to be 379.1 nm. What transition does it correspond to?

4-3. An astronomer finds a new absorption line with $\lambda = 164.1$ nm in the ultraviolet region of the sun's continuous spectrum. He attributes the line to hydrogen's Lyman series. Is he right? Justify your answer.

4-4. The series of hydrogen spectral lines with $m = 4$ is called Brackett's series. Compute the wavelengths of the first four lines of Brackett's series.

4-5. In a sample that contains hydrogen, among other things, four spectral lines are found in the infrared with wavelengths 7460 nm, 4654 nm, 4103 nm, and 3741 nm. Which one does not belong to a hydrogen spectral series?

Section 4-2 Rutherford's Nuclear Model

4-6. A gold foil of thickness 2.0 μm is used in a Rutherford experiment to scatter α particles with energy 7.0 MeV. (*a*) What fraction of the particles will be scattered at angles greater than 90°? (*b*) What fraction will be scattered at angles between 45° and 75°? (For gold, $\rho = 19.3$ g/cm^3 and $M = 197$ g/mol.)

4-7. (*a*) What is the ratio of the number of particles per unit area on the screen scattered at 10° to those at 1°? (*b*) What is the ratio of those scattered at 30° to those at 1°?

4-8. For α particles of 7.7 MeV (those used by Geiger and Marsden), what impact parameter will result in a deflection of 2° for a thin gold foil?

4-9. What will be the distance of closest approach r_d to a gold nucleus for an α particle of 5.0 MeV? 7.7 MeV? 12 MeV?
4-10. What energy α particle would be needed to just reach the surface of an Al nucleus if its radius is 4 fm?
4-11. If a particle is deflected by 0.01° in each collision, about how many collisions would be necessary to produce an rms deflection of 10°? (Use the result from the one-dimensional random walk problem in statistics stating that the rms deflection equals the magnitude of the individual deflections times the square root of the number of deflections.) Compare this result with the number of atomic layers in a gold foil of thickness 10^{-6} m, assuming that the thickness of each atom is 0.1 nm = 10^{-10} m.
4-12. Consider the foil and α particle energy in Problem 4-6. Suppose that 1000 of those particles suffer a deflection of more than 25°. (*a*) How many of these are deflected by more than 45°? (*b*) How many are deflected between 25° and 45°? (*c*) How many are deflected between 75° and 90°?

Section 4-3 The Bohr Model of the Hydrogen Atom

4-13. The radius of the $n = 1$ orbit in the hydrogen atom is $a_0 = 0.053$ nm. (*a*) Compute the radius of the $n = 6$ orbit. (*b*) Compute the radius of the $n = 6$ orbit in singly ionized helium (He^+), which is hydrogenlike.
4-14. Show that Equation 4-19 for the radius of the first Bohr orbit and Equation 4-20 for the magnitude of the lowest energy for the hydrogen atom can be written as

$$a_0 = \frac{hc}{\alpha mc^2} = \frac{\lambda_c}{2\pi\alpha}$$
$$E_1 = \tfrac{1}{2}\alpha^2 mc^2$$

where $\lambda_c = h/mc$ is the Compton wavelength of the electron and $\alpha = ke^2/\hbar c$ is the fine-structure constant. Use these expressions to check the numerical values of the constants a_0 and E_1.
4-15. Calculate the three longest wavelengths in the Lyman series ($n_f = 1$) in nm, and indicate their position on a horizontal linear scale. Indicate the series limit (shortest wavelength) on this scale. Are any of these lines in the visible spectrum?
4-16. If the angular momentum of Earth in its motion around the sun were quantized like a hydrogen electron according to Equation 4-17, what would Earth's quantum number be? How much energy would be released in a transition to the next lowest level? Would that energy release (presumably as a gravity wave) be detectable? What would be the radius of that orbit? (The radius of Earth's orbit is 1.50×10^{11} m.)
4-17. Light of wavelength 410.7 nm is observed in emission from a hydrogen source. (*a*) What transition between hydrogen Bohr orbits is responsible for this radiation? (*b*) To what series does this transition belong?
4-18. An atom in an excited state will on the average undergo a transition to a state of lower energy in about 10^{-8} s. If the electron in a doubly ionized lithium atom (Li^{2+}, which is hydrogenlike) is placed in the $n = 4$ state, about how many revolutions around the nucleus does it make before undergoing a transition to a lower energy state?
4-19. It is possible for a muon to be captured by a proton to form a muonic atom. A muon is identical to an electron except for its mass, which is 105.7 MeV/c^2. (*a*) Calculate the radius of the first Bohr orbit of a muonic atom. (*b*) Calculate the magnitude of the lowest energy. (*c*) What is the shortest wavelength in the Lyman series for this atom?
4-20. In the lithium atom ($Z = 3$) two electrons are in the $n = 1$ orbit and the third is in the $n = 2$ orbit. (Only two are allowed in the $n = 1$ orbit because of the exclusion principle, which will be discussed in Chapter 7.) The interaction of the inner electrons with the outer one can be approximated by writing the energy of the outer electron as

$$E = -Z'^2 \frac{E_1}{n^2}$$

where $E_1 = 13.6$ eV, $n = 2$, and Z' is the effective nuclear charge, which is less than 3 because of the screening effect of the two inner electrons. Using the measured ionization energy of 5.39 eV, calculate Z'.
4-21. Draw to careful scale an energy-level diagram for hydrogen for levels with $n = 1$, 2, 3, 4, ∞. Show the following on the diagram: (*a*) the limit of the Lyman series, (*b*) the H_β line, (*c*) the transition between the state whose binding energy (= energy needed to remove the electron from the atom) is 1.51 eV and the state whose excitation energy is 10.2 eV, and (*d*) the longest wavelength line of the Paschen series.
4-22. A hydrogen atom at rest in the laboratory emits the Lyman α radiation. (*a*) Compute the recoil kinetic energy of the atom. (*b*) What fraction of the excitation energy of the $n = 2$ state is carried by the recoiling atom? (*Hint:* Use conservation of momentum.)
4-23. What is the radius of the $n = 1$ orbit in C^{5+}? What is the energy of the electron in that orbit? What is the wavelength of the radiation emitted by C^{5+} in the Lyman α transition?
4-24. The electron-positron pair that was discussed in Chapter 2 can form a hydrogenlike system called *positronium*. Calculate (*a*) the energies of the three lowest states and (*b*) the wavelength of the Lyman α and β lines. (Detection of those lines is a "signature" of positronium formation.)
4-25. With the aid of tunable lasers, Rydberg atoms of sodium have been produced with $n \approx 100$. The resulting atomic diameter would correspond in hydrogen to $n \approx 600$. (*a*) What would be the diameter of a hydrogen atom whose electron is in the $n \approx 600$ orbit? (*b*) What would be the speed of the electron in that orbit? (*c*) How does the result in (*b*) compare with the speed in the $n \approx 1$ orbit?

Section 4-4 X-Ray Spectra

4-26. (*a*) Calculate the next two longest wavelengths in the *K* series (after the K_α line) of molybdenum. (*b*) What is the wavelength of the shortest wavelength in this series?
4-27. The wavelength of the K_α x-ray line for an element is measured to be 0.0794 nm. What is the element?
4-28. The L_α line for a certain element has a wavelength of 0.3617 nm. What is the element?
4-29. What is the approximate radius of the $n = 1$ orbit of gold ($Z = 79$)? Compare this with the radius of the gold nucleus, about 7.1 fm.
4-30. What is the minimum potential that must be applied across an x-ray tube in order to observe the (*a*) K_α line of tungsten, (*b*) the K_α line of copper, and (*c*) the L_α line of copper? What is the λ_{min} of the continuous spectrum in each case?
4-31. In a particular x-ray tube, an electron approaches the target moving at 2.25×10^8 m/s. It slows down on being deflected by a nucleus of the target, emitting a photon of energy 32.5 keV. Ignoring the nuclear recoil, but not relativity, compute the final speed of the electron.
4-32. (*a*) Compute the energy of an electron in the $n = 1$ (*K* shell) of tungsten, using $Z - 1$ for the effective nuclear charge. (*b*) The experimental result for this energy is 69.5 keV. Assume that the effective nuclear charge is $(Z - \sigma)$, where σ is called the screening constant, and calculate σ from the experimental result.
4-33. Construct a Moseley plot similar to Figure 4-18 for the K_β x rays of the elements listed (the x-ray energies are given in keV):

Al 1.56	Ar 3.19	Sc 4.46	Fe 7.06
Ge 10.98	Kr 14.10	Zr 17.66	Ba 36.35

Determine the slope of your plot, and compare it with the K_β line in Figure 4-18.

Section 4-5 The Franck-Hertz Experiment

4-34. Suppose that, in a Franck-Hertz experiment, electrons of energy up to 13.0 eV can be produced in the tube. If the tube contained atomic hydrogen, (*a*) what is the shortest-wavelength spectral line that could be emitted from the tube? (*b*) List all of the hydrogen lines that can be emitted by this tube.

4-35. Using the data in Figure 4-23*b* and a good ruler, draw a carefully scaled energy-level diagram covering the range from 0 eV to 60 eV for the vibrational states of this solid. What approximate energy is typical of the transitions between adjacent levels corresponding to the larger of each pair of peaks?

4-36. The transition from the first excited state to the ground state in potassium results in the emission of a photon with $\lambda = 770$ nm. If potassium vapor is used in a Franck-Hertz experiment, at what voltage would you expect to see the first decrease in current?

4-37. If we could somehow fill a Franck-Hertz tube with positronium, what cathode-grid voltage would be needed to reach the second current decrease in the positronium equivalent of Figure 4-22? (See Problem 4-24.)

4-38. Electrons in the Franck-Hertz tube can also have elastic collisions with the Hg atoms. If such a collision is head on, what fraction of its initial kinetic energy will an electron lose, assuming the Hg atom to be at rest? If the collision is not head on, will the fractional loss be greater or less than this?

Section 4-6 Critique of Bohr Theory and of the "Old" Quantum Mechanics

There are no problems for this section.

Level II

4-39. Derive Equation 4-8 along the lines indicated in the paragraph that precedes it.

4-40. Geiger and Marsden used α particles with 7.7-MeV kinetic energy and found that when they were scattered from thin gold foil, the number observed to be scattered at all angles agreed with Rutherford's formula. Use this fact to compute an upper limit on the radius of the gold nucleus.

4-41. (*a*) The current i due to a charge q moving in a circle with frequency f_{rev} is qf_{rev}. Find the current due to the electron in the first Bohr orbit. (*b*) The magnetic moment of a current loop is iA, where A is the area of the loop. Find the magnetic moment of the electron in the first Bohr orbit in units A · m². This magnetic moment is called a *Bohr magneton.*

4-42. Use a spreadsheet to calculate the wavelengths (in nm) of the first five spectral lines of the Lyman, Balmer, Paschen, and Brackett series of hydrogen. Show the positions of these lines on a linear scale and indicate which ones lie in the visible.

4-43. Show that a small change in the reduced mass of the electron produces a small change in the wavelength of a spectral line given by $\Delta\lambda/\lambda = -\Delta\mu/\mu$. Use this to calculate the difference $\Delta\lambda$ in the Balmer red line $\lambda = 656.3$ nm between hydrogen and deuterium, which has a nucleus with twice the mass of hydrogen.

4-44. A beam of 10-MeV protons is incident on a thin aluminum foil of thickness 10^{-6} m. Find the fraction of the particles that are scattered through angles greater than (*a*) 10° and (*b*) 90°.

4-45. The Li^{2+} ion is essentially identical to the H atom in Bohr's theory, aside from the effect of the different nuclear charges and masses. (*a*) What transitions in Li^{2+} will yield emission lines whose wavelengths are very nearly equal to the first two lines of the Lyman series in hydrogen? (*b*) Calculate the difference between the wavelength of the Lyman α line of hydrogen and the emission line from Li^{2+} that has very nearly the same wavelength.

4-46. In an α scattering experiment, the area of the α particle detector is 0.50 cm². The detector is located 10 cm from a 1.0-μm-thick silver foil. The incident beam carries a current of 1.0 nA, and the energy of each α particle is 6.0 MeV. How many α particles will be counted per second by the detector at (*a*) $\theta = 60°$? (*b*) $\theta = 120°$?

4-47. The K_α, L_α, and M_α x rays are emitted in the $n = 2 \rightarrow n = 1$, $n = 3 \rightarrow n = 2$, and $n = 4 \rightarrow n = 3$ transitions, respectively. For calcium ($Z = 20$) the energies of these transitions are 3.69 keV, 0.341 keV, and 0.024 keV, respectively. Suppose that energetic photons impinging on a calcium surface cause ejection of an electron from the K shell of the surface atoms. Compute the energies of the Auger electrons that may be emitted from the L, M, and N shells ($n = 2$, 3, and 4) of the sample atoms, in addition to the characteristic x rays.

4-48. Figure 3-18*b* shows the K_α and K_β characteristic x rays emitted by a molybdenum (Mo) target in an x-ray tube whose accelerating potential is 35 kV. The wavelengths are $K_\alpha = 0.071$ nm and $K_\beta = 0.063$ nm. (*a*) Compute the corresponding energies of these photons. (*b*) Suppose we wish to prepare a beam consisting primarily of K_α x rays by passing the molybdenum x rays through a material that absorbs K_β x rays more strongly than K_α x rays by photoelectric effect on K-shell electrons of the material. Which of the materials listed in the accompanying table with their K-shell binding energies would you choose? Explain your answer.

Element	Zr	Nb	Mo	Tc	Ru
Z	40	41	42	43	44
E_K (keV)	18.00	18.99	20.00	21.04	22.12

Level III

4-49. A small shot of negligible radius hits a stationary smooth, hard sphere of radius R, making an angle β with the normal to the sphere, as shown in Figure 4-24. It is reflected at an equal angle to the normal. The scattering angle is $\theta = 180° - 2\beta$, as shown. (*a*) Show by the geometry of the figure that the impact parameter b is related to θ by $b = R \cos \frac{1}{2}\theta$. (*b*) If the incoming intensity of the shot is I_0 particles/s · area, how many are scattered through angles greater than θ? (*c*) Show that the cross section for scattering through angles greater than 0° is πR^2. (*d*) Discuss the implication of the fact that the Rutherford cross section for scattering through angles greater than 0° is infinite.

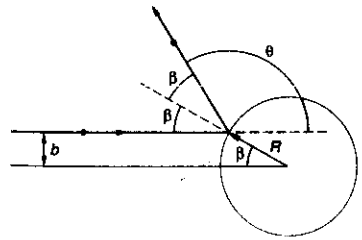

Fig. 4-24 Small particle scattered by a hard sphere of radius R.

4-50. Singly ionized helium He^+ is hydrogenlike. (*a*) Construct a carefully scaled energy-level diagram for He^+ similar to that in Figure 4-16, showing the levels for $n = 1$, 2, 3, 4, 5, and ∞. (*b*) What is the ionization energy of He^+? (*c*) Compute the difference in wavelength between each of the first two lines of the Lyman series of hydrogen and the first two lines of the He^+ Balmer series. Be sure to include the reduced mass correction for both atoms. (*d*) Show that for every spectral line of hydrogen, He^+ has a spectral line of very nearly the same wavelength. (Mass of $He^+ = 6.65 \times 10^{-27}$ kg.)

4-51. Listed in the table are the L_α x-ray wavelengths for several elements. Construct a Moseley plot from these data. Compare the slope with the appropriate one in Figure 4-18. Determine and interpret the intercept on your graph, using a suitably modified version of Equation 4-35.

Element	P	Ca	Co	Kr	Mo	I
Z	15	20	27	36	42	53
Wavelength (nm)	10.41	4.05	1.79	0.73	0.51	0.33

4-52. In this problem you are to obtain the Bohr results for the energy levels in hydrogen without using the quantization condition of Equation 4-17. In order to relate Equation 4-14 to the Balmer-Ritz formula, assume that the radii of allowed orbits are given by $r_n = n^2 r_0$, where n is an integer and r_0 is a constant to be determined. (*a*) Show that the frequency of radiation for a transition to $n_f = n - 1$ is given by $f \approx kZe^2/hr_0n^3$ for large n. (*b*) Show that the frequency of revolution is given by

$$f_{rev}^2 = \frac{kZe^2}{4\pi^2 m\, r_0^3 n^6}$$

(*c*) Use the correspondence principle to determine r_0 and compare with Equation 4-19.

4-53. Calculate the energies and speeds of electrons in circular Bohr orbits in a hydrogenlike atom using the relativistic expressions for kinetic energy and momentum.

4-54. (*a*) Write a computer program for your personal computer or programmable calculator that will provide you with the spectral series of H-like atoms. Inputs to be included are n_i, n_f, Z, and the nuclear mass M. Outputs are to be the wavelengths and frequencies of the first six lines and the series limit for the specified n_f, Z, and M. Include the reduced mass correction. (*b*) Use the program to compute the wavelengths and frequencies of the Balmer series. (*c*) Pick an $n_f > 100$, name the series the [your name] series, and use your program to compute the wavelengths and frequencies of the first three lines and the limit.

4-55. Figure 4-25 shows an energy-loss spectrum for He measured in an apparatus such as that shown in Figure 4-23*a*. Use the spectrum to construct and draw carefully to scale an energy-level diagram for He.

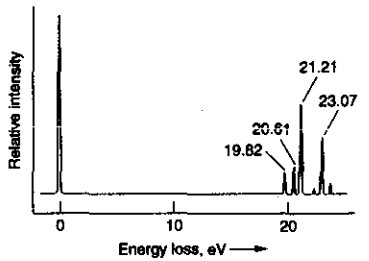

Fig. 4-25 Energy-loss spectrum of helium. Incident electron energy was 34 eV. The elastically scattered electrons cause the peak at 0 eV.

4-56. If electric charge did not exist and electrons were bound to protons by the gravitational force to form hydrogen, derive the corresponding expressions for a_0 and E_n and compute the energy and frequency of the H_α line and the limit of the Balmer series. Compare these with the corresponding quantities for "real" hydrogen.

4-57. A sample of hydrogen atoms are all in the $n = 5$ state. If all the atoms return to the ground state, how many different photon energies will be emitted, assuming all possible transitions occur? If there are 500 atoms in the sample and assuming that from any state all possible downward transitions are equally probable, what is the total number of photons that will be emitted when all of the atoms have returned to the ground state?

Chapter 5 The Wavelike Properties of Particles

In 1924, a French graduate student, Louis de Broglie,[1] proposed in his doctoral dissertation that the dual—i.e., wave-particle—behavior that was by then known to exist for radiation was also a characteristic of matter, in particular, electrons. This suggestion was highly speculative, since there was yet no experimental evidence whatsoever for any wave aspects of electrons or any other particles. What had led him to this seemingly strange idea? It was a "bolt out of the blue," like Einstein's "happy thought," that led to the principle of equivalence (see Chapter 2). De Broglie described it with these words:

> After the end of World War I, I gave a great deal of thought to the theory of quanta and to the wave-particle dualism. . . . It was then that I had a sudden inspiration. Einstein's wave-particle dualism was an absolutely general phenomenon extending to all physical nature.[2]

Since the visible universe consists entirely of matter and radiation, de Broglie's hypothesis is a fundamental statement about the grand symmetry of nature. (There is currently strong observational evidence that approximately 70 percent of the universe consists of some sort of invisible "dark energy." See Chapter 14.)

5-1 The de Broglie Hypothesis

De Broglie stated his proposal mathematically with the following equations for the frequency and wavelength of the electron waves, which are referred to as the *de Broglie relations:*

$$f = \frac{E}{h} \qquad \textbf{5-1}$$

$$\lambda = \frac{h}{p} \qquad \textbf{5-2}$$

where E is the total energy, p is the momentum, and λ is called the *de Broglie wavelength* of the particle. For photons, these same equations result directly from